Fall 2019

Modeling Climate-Dependent Larval Growth Rate and Duration of Olympia oysters in the Salish Sea

Jake A. Lawlor
Western Washington University, jakealawlor@gmail.com

Modeling Climate-Dependent Larval Growth Rate and Duration of Olympia oysters in the Salish Sea

By

Jake Lawlor

Accepted in Partial Completion
of the Requirements for the Degree
Master of Science

ADVISORY COMMITTEE

Chair, Dr. Shawn Arellano

Dr. Benjamin Miner

Dr. Brooke Love

GRADUATE SCHOOL

David L. Patrick, Interim Dean

Master's Thesis

In presenting this thesis in partial fulfillment of the requirements for a master's degree at Western Washington University, I grant to Western Washington University the non-exclusive royalty-free right to archive, reproduce, distribute, and display the thesis in any and all forms, including electronic format, via any digital library mechanisms maintained by WWU.

I represent and warrant this is my original work, and does not infringe or violate any rights of others. I warrant that I have obtained written permissions from the owner of any third party copyrighted material included in these files.

I acknowledge that I retain ownership rights to the copyright of this work, including but not limited to the right to use all or part of this work in future works, such as articles or books. Library users are granted permission for individual, research and non-commercial reproduction of this work for educational purposes only. Any further digital posting of this document requires specific permission from the author.

Any copying or publication of this thesis for commercial purposes, or for financial gain, is not allowed without my written permission

Jake Lawlor

December 2nd, 2019

Modeling Climate-Dependent Larval Growth Rate and Duration of Olympia oysters in the Salish Sea

A Thesis
Presented to
The Faculty of
Western Washington University

In Partial Fulfillment
Of the Requirements for the Degree
Master of Science

By
Jake A. Lawlor
December 2019

Abstract

Most invertebrates in the ocean begin their lives with a planktonic larval phase that is of utmost importance for dispersal and distribution of these species, especially for organisms that are sessile or otherwise mobility-limited during adult life. As larvae are particularly vulnerable to environmental change, holistic understanding of interacting climate stressors on larval life is important to predict population persistence and vulnerability of species. However, traditional experimental designs are often limited by resolution in understanding multiple stress relationships, as environmental variables in the ocean do not occur in discrete interacting levels. Here, I use a novel experimental approach to model growth rate and duration of Olympia oyster larvae and predict the suitability of habitats for larval survival in interacting gradients of temperature, salinity, and ocean acidification. I find that temperature and salinity are closely linked to larval growth and larval habitat suitability, but larvae are resistant to acidification. Olympia oyster larvae from populations in the Salish Sea exhibit higher growth rate and greater tolerance to habitats in near-future climate change conditions compared to present-day conditions in the Salish Sea, suggesting that this species will benefit from some degree of global ocean change. Using generalized linear modeling, I predict larval growth and duration in present-day and future oceanographic conditions in the Salish Sea, finding a vast decrease in mean pelagic larval duration by the year 2095. Using these data, I explore implications of these relationships for Olympia oysters across their range now and in the future.

Acknowledgements

This work would not have been possible without the guidance and leadership of my thesis advisor, Dr. Shawn Arellano. Thank you for supporting me in all my endeavors, for pushing me to follow my interests, and for allowing me to grow in confidence and capability in your lab. Thank you to my thesis committee, Drs. Ben Miner and Brooke Love, for your guidance and your open doors, and to Drs. Brian Bingham and Sylvia Yang for additional help along the way.

I would also like to thank Brooke McIntyre, who devoted her time and her positivity through long sampling days, as well as everyone who volunteered their time to help during the process. This includes Abby Ernest-Beck, Katie Mills-Orcutt, Amanda Stromecki, Maizer Sparkman, Jasper Paisner, Annalee McBrady, Cristina Villalobos, Holly Flann, Lillian Kuehl, Mike Rose, and Mackenna Newmarch. I would also like to thank Ryan Crim and the Puget Sound Restoration Fund team for providing larvae and other supplies for this experiment and preliminary trials. Thank you to Tarang Khangaonkar for sharing his Salish Sea Model outputs and his guidance on how to utilize them.

Finally, thank you to my family for their support and encouragement through my academic life and career.

This research was supported by National Science Foundation grant #1538626, and research funds from Western Washington University.

Table of Contents

Abstract iv

Acknowledgements v

List of Tables vii

List of Figures viii

Introduction 1

Methods 5

Experimental Design 5

Spawning and larval rearing 6

Data collection 7

Analysis 8

Predicting Impacts in the Salish Sea 9

Results 12

Treatment Values 12

Larval Growth 12

Larval Habitat Suitability 14

Predicting Impacts in the Salish Sea 14

Discussion 16

Climate stress and larval performance 16

Model validity in the Salish Sea 19

Ostrea lurida, climate, and ecological theory 21

Tables and Figures 25

References 36

Supplementary Materials 42

List of Tables

Table 1: Model summary of Generalized Linear Model for larval growth, using temperature and salinity as predictor variables for larval growth rate 25

Table 2: Model summary of multiple logistic regression model of treatment habitat suitability for Olympia oyster larvae using temperate and salinity as predictor variables for suitability. ... 26

Table 3: Mean temperature and salinity from the Salish Sea Hydrodynamic Model from July 5-August 23 2014 and 2095 in the 19 state-managed Olympia oyster restoration sites in Washington State with average model-predicted PLD in each site for each year. Last column shows change in projected PLD in each site for each year. Last column shows change in projected PLD between 2014 and 2095 conditions. 27

Supplementary Table 1: Values for 50 experimental treatments averaged over the duration of each cup's involvement in the experiment (3-17 days) with ± SD for each value. 42

Supplementary Table 2: Model selection process for growth model. Larval growth rate (Gr) is predicted using temperature (Temp), salinity (Sal), pH, pCO_2, and aragonite saturation (Ar). Bolded text in the model formulas represents predictors with individual p values <0.05. AIC, BIC, and R^2 were primarily used for model comparison. The last model listed is the final model chosen. 43

Supplementary Table 3: Model selection for habitat suitability. Suitability was modeled with a binomial family logistic multiple regression using temperature (Temp), salinity (Sal), pH, pCO_2, and aragonite saturation (Ar) as predictor variables. Bolded text in model formulas signifies individual predictor p values <0.05. Model comparisons used AIC, BIC, and Pseudo R^2. The last model listed is the final chosen model for habitat suitability. 44

Supplementary Table 4: Case study field data from two restoration sites in Washington State between the years 2014 and 2019. Field data are listed on the left, and modeled response variables on the right of the vertical line. "SEA" label denotes data sourced from the WWU SEA Discovery Center in Poulsbo, WA. "McIntyre" signifies from McIntyre et al (in revision), and "Cordoba" from Cordoba and Arellano, unpublished data. 45

List of Figures

Figure 1: Growth experiment scheme. The culturing tank had inflow on the left end, direction flow towards the right, and four 500W digital submersible aquarium heaters heating the water as it flowed into each new chamber. Each heat chamber contains 10 culture cups, each randomly assigned a CO_2 value of 400, 800, 1200, or 1600 ppm, and a salinity value from 12-39PSU in units of three. All four CO_2 values and ten salinity values are present within each 10-cup temperature group. 28

Figure 2: Average treatment values of culture cups in the experiment. X and Y axes represent mean salinity and temperature, color represents average pH. Error bars represent standard deviation of temperature and salinity for the duration of the cup's inclusion in the experiment (3-17 days). Average standard deviation of salinity was ±0.59 PSU, temperature was ±0.83°C, and pH was ±0.03 pH units. 29

Figure 3: Size values through time of all larvae across experimental treatments. a) larval sizes in all treatment cups where black dots represent non-competent larvae (lacking a visible eyespot) and red dots represent competent larvae. b) average sizes with error bars ±SD for larval treatment cups. Red dots represent samples where over 25% or larvae sampled were visibly competent. In both plots, the horizontal line at 260µm represents the size at which I considered larvae late-stage veligers. 30

Figure 4: Growth of oyster larvae in 50 climate treatments arranged by target salinity (left-right) and target temperature (bottom-top). Black lines are lengths of larval shells (n=3-44), white lines are linear regressions, showing average growth/day. Horizontal dotted line represents late-stage larva size (260µm). Filled in circles represent proportion of sampled larvae with visible eyespots at all samples >25%. Vertical dotted lines indicate >95% mortality. Panel color represents growth rate (µm/day). Numbers denote theoretical first sampling of >25% eyed larvae in each cup. 31

Figure 5 a) Gridded Bivariate Interpolation of growth rate between experimental temperature and salinity coordinates, overlaid with real values of growth rate in experimental treatment points. b) Predicted growth rate using Generalized Linear Model function at every salinity (9-39PSU) and temperature (11-30°C) combination with experimental treatments overlaid. Color inside points represents real growth rate in given experimental treatment, while color of the panel represents modeled growth rate. Outline colors of points and error bars represent the absolute difference between real and predicted growth, where red outlined points are more poorly predicted by the model. 32

Figure 6 : Habitat suitability likelihood of experimental treatments for Olympia oyster larvae. a) Predicted habitat suitability in 50 environmental treatments. Treatments above the horizontal line are predicted as survivable. Color represents actual suitability in experimental treatments. b) GLM-predicted likelihood of suitability across salinity (9-39PSU) and temperature (11-30°C).

Color represents percent likelihood of 25% or more larvae in given environmental conditions growing to competency. 33

Figure 7: Predicted growth rate using Generalized Linear Model larval growth function with averaged temperature and salinity coordinates of 19 state-managed Olympia oyster restoration sites from July 5 – August 23 2014 (blue triangles) and 2095 (red circles) calculated from values in the Salish Sea Hydrodynamic Model. Black diamonds represent average values measured in two bays of restoration focus. White numbered contour lines represent likelihood that treatment will be suitable larval habitat. Inset shows site locations in the Salish Sea. 34

Figure 8 : Predicted pelagic larval duration of oysters released in each of the 19 state-managed restoration sites for the species in Washington State ordered North-South in the Salish Sea. Points represent time for simulated larvae to grow from release size(156µm) to competence size (260µm) in averaged values temperature and salinity values from hourly timepoints from July 4 – August 23, 2014 (blue triangles) and 2095 (red circles). Horizontal lines represent average duration in PLD over all sites in each year. Vertical arrows show change in projected PLD from 2014 to 2095. 35

Supplementary Figure 1: Treatment cup variable stability over time from May 7 to May 21, 2018. 45

Supplementary Figure 2: Correlation matrix of predictor variables in larval growth and habitat suitability models. 46

Supplementary Figure 3: average treatment values of culture cups in the experiment organized by temperature and pH (a), and pH and salinity (b) as addendum to Fig 2, arranged by salinity and temperature. Error bars represent the standard deviation of axis variables for the duration of the cup's inclusion in the experiment (3-17 days). 47

Supplementary Figure 4: Experimental growth rate distribution by variable with loess curve fits. 49

Introduction

Many marine invertebrates begin their lives as tiny planktonic larvae that drift in the water column and disperse away from their parents. For sessile species, these larval periods are especially important as they are the only times throughout life history during which organisms are capable of dispersal. As such, survival during the larval phase is critical for the persistence of populations. The vast majority of larvae do not live to competence, and larvae are highly sensitive to environmental conditions (Byrne 2011; Pineda et al. 2012), so patterns of larval survival and metamorphosis along environmental gradients are closely related to population demographics and geographic distributions of species (Gaines & Roughgarden 1985; Pecorino et al. 2013). Responses of early life history stages to environmental conditions help to explain and predict the structures of communities in coastal oceans.

Understanding environmental influence on life history bottlenecks is particularly important as climate variables that affect fitness are rapidly changing. Though the list of anthropogenically-influenced climate variables is broad and regionally variable, three of the most important environmental factors to consider are ocean temperature, acidification, and salinity. Broadly, temperature influences metabolism in ectotherms, and thermal tolerances largely dictate distributions of marine organisms (Pörtner & Farrell 2008); changes in temperature can cause changes in species developmental rate and survival that delimit range boundaries of species (O'Connor et al. 2007; Sunday et al. 2012). Acidification, or the shift of carbonate chemistry of a system, can affect calcification of animals with carbonate skeletons (Doney et al. 2009; Fabry et al. 2008) and, thus, will disproportionately affect many essential ecosystem engineers in marine systems such as corals, bivalves, and crabs (Kroeker et al. 2010).

Changes in ocean salinity affect cellular processes such as osmotic regulation and respiration in marine animals (Beadle 1931). Further, these stressors interact in coastal environments, and impacts of combined stressors often operate synergistically, highlighting the importance of studying stressors in combination (Byrne & Przeslawski 2013; Kroeker et al. 2013; Przeslawski et al. 2015). By the year 2100, climate models predict between 2 and 5°C rise in sea surface temperatures, a pH drop of up to 0.4 pH units, and more frequent pulses of freshwater in coastal regions (Feely et al. 2009; IPCC 2019; Rhein et al. 2013). Better understanding of how these changes will influence marine species is increasingly important for conservation and resource management in this time of rapid global change.

Here, I analyze interacting influences of temperature, salinity, and acidification on larvae of the Olympia oyster, *Ostrea lurida*. Oysters are calcifying invertebrates that depend solely on the larval phase for dispersal and they have immense ecological and economic importance. Therefore, oysters make pertinent models for climate change studies (Narita et al. 2012). *Ostrea lurida,* specifically, is a species of key regional concern on the U.S. west coast. After decades of overharvesting, pollution, and habitat loss, populations have been depleted to a small fraction of their historical numbers (Beck et al. 2011). In Washington state, the Department of Fish and Wildlife, in collaboration with Tribal governments and conservation NGOs, has identified 19 restoration sites for the species, with the goal of repopulating selected bays with self-sustaining Olympia oyster populations (Blake & Bradbury 2012). Restoration efforts include out-planting of hatchery-raised seed into restoration sites, but because further establishment of populations relies on natural larval setting, predicting environments in which

larvae can thrive will help to predict future success of populations and target restoration efforts.

I tested environmental influence on growth rate and pelagic larval duration (PLD), or the time between release and settlement, of *O. lurida* larvae. I also assessed larval habitat suitability in terms of environmental parameter thresholds necessary for larval survival. Because growth rate and PLD determine the timeframe over which larvae can access ocean currents, changes in these factors influence the dispersal potential and population connectivity of sessile species (Pineda et al. 2007; Shanks 2009). This can lead to decreased genetic diversity and increased fragmentation of metapopulations. Larval habitat suitability outlines the maximum extent of a species' distribution in any given spawn season, as larvae are typically more sensitive to environmental stress than adult stages (Byrne 2011; Pineda et al. 2012). Although certain habitat conditions may support adult oysters, if those conditions do not support survival of larvae to competency, those habitats will fail as sources of larvae for dispersal, or as sites for new adult populations.

In bivalves, we generally expect acidification to reduce growth rate and increase PLD (Hettinger et al. 2013; Kroeker et al. 2010; Li et al. 2014; Talmage & Gobler 2011; Waldbusser et al. 2015), warming to reduce PLD but have variable effects on growth (Dekshenieks et al. 1993; O'Connor et al. 2007; Talmage & Gobler 2011), and hyposalinity to decrease growth and increase PLD (Ko et al. 2014). Suitability of habitats to facilitate larval survival to competence generally decreases with acidification (Barros et al. 2013; Barton et al. 2015; Hettinger et al. 2012; Kroeker et al. 2010; Talmage & Gobler 2011), decreases with warming (Talmage & Gobler 2011), and decreases at low salinities (Ko et al. 2014; Wasson et al. 2016). However,

interactions between stressors can be complex (Cole et al. 2016; Ko et al. 2014), and traditional multifactorial experimental designs often do not capture the full complexity of functional responses between selected environmental treatment levels.

Because conditions in the ocean do not occur isolation or at discrete levels, I employ a novel experimental design to test larvae in interacting gradients of environmental conditions. Using fifty unique experimental treatments all housed in one tank, I test impacts of temperature, salinity, and acidification on *O. lurida* larvae. This unique design allows me to address continuous functional response patterns across environmental gradients while avoiding many issues of pseudoreplication associated with multi-factor studies (Havenhand et al. 2010). Using Generalized Linear Models for growth and environmental habitat suitability derived from these experimental data, I predict larval growth and habitat suitability under current conditions in the Salish Sea, and as environmental conditions continue to change.

Methods

Experimental Design

I designed a custom heat-gradient culturing tank allowing for larval culturing in 50 unique combinations of temperature, salinity, and pCO_2. The tank featured directional flow, guaranteed by the placement of a series of weirs directing water through five heating chambers, where 500W digital submersible aquarium heaters raised temperature of the seawater before moving across the next weir (Fig 1). These five stable heat levels ranged from approximately 13°C at the inflow to 28°C on exit. Within each heat level, ten 32-oz polyethylene SOLO brand cups filled with 800ml treatment water were randomly assigned one of ten salinity values (12-39, in intervals of 3). Each cup was bubbled with one of four pCO_2 concentration air treatments (400, 800, 1200, and 1600ppm pCO_2 air), with temperature- and salinity-driven differences in solubility ensuring a gradient of achieved carbonate chemistry conditions between treatments. Every salinity and pCO_2 level was present in each 10-cup temperature group. Salinities were achieved by manually mixing preequilibrated 0.35µm filtered seawater (FSW) with concentrated brine (FSW enhanced with Marine Mix instant ocean salt) or bicarbonate-enriched deionized water simulating alkalinity levels of freshwater inputs in the region (Long & Khangaonkar 2014). Acidification was achieved by individually bubbling CO_2 controlled air into treatment cultures using an air compressor, CO_2 scrubber, and eight mass flow controllers mixing pure CO_2 with CO_2-free air for treatment conditions (system described in Love et al. 2017). The non-uniform multifactorial spread of this design allowed me to analyze

predictor variables as continuous gradients and interpolate responses between treatment values, rather than conduct treatment level comparisons. Because all culture cups were housed in one tank, I avoided many random effects that I could have faced by splitting my treatments into a limited number of incubators. It is important to note that some pseudoreplication issues persisted in this design through shared pCO_2 tubes and row alignment within the culturing tank. Still, I designed this tank to simulate samples from 50 independent field sites, so I measured and analyzed them as such.

Spawning and larval rearing

All larvae for this experiment were provided by the Puget Sound Restoration Fund oyster hatchery in Port Orchard, Washington. Broodstock were collected from Mud Bay, Washington, and used in one hatchery spawn season. Broodstock from separate spawning groups were consolidated into one tank and held together for one week before larval collection. Larvae were released and collected on May 3, 2018, concentrated on a moist Nitex mesh, and shipped on ice overnight to Shannon Point Marine Center in Anacortes, Washington. Larvae were distributed into treatment cups at a target density of 2 larvae/ml on May 4, 2018. Each Monday, Wednesday, and Friday, larvae were poured from culture cups onto 100µm Nitex screens for full water changes with preequilibrated treatment water then fed a diet of *Isochrysis galbana* at 100,000 cells/ml. While the environmental conditions manipulated in my treatment cups could potentially affect the nutritional content of algae, I chose to use *I. galbana* as food due to its common utilization in environmental stress studies (Cole et al. 2016; Hettinger et al. 2013; Ko et al. 2013, 2014; Talmage & Gobler 2011). Additionally, because I fed

each culture following water changes three times per week from control condition algae cultures, larvae should have had the opportunity to consume algae before environmental conditions significantly affected its nutrient content. During the time larvae were condensed on screens, samples were collected to measure growth and assess mortality (see next section).

Data collection

Three times per week, water chemistry, and larval size, developmental stage, and mortality were assessed in each culture cup. I used an Orion Star A329 multimeter to measure water temperature and salinity prior to water changes, and filtered water samples into 20ml scintillation vials that I fixed with 20µl mercuric chloride for later pH and DIC analysis. Fixed samples were later measured for pH using an Ocean optics S-UV-VIS flame spectrophotometer, measured in a 5cm jacketed cuvette for a baseline spectrum, then again after addition of 20µl m-cresol dye (Dickson et al. 2007). DIC was measured with an Apollo SciTech AS-C3 DIC Analyzer, calibrated to a standard curve built from varying volumes of certified reference material (CRM, Batch 149, Dickson, Scripps Institute of Oceanography). I used measured pH and DIC values to calculate pCO2, pH (total scale) and aragonite saturation states (Ω) in each culture cup for each sampling event using CO2SYS (Pelletier et al. 2012) with K1 and K2 equilibrium constants (Millero et al. 2006).

To assess mortality and competency, and to take samples for larval morphology measurements, I sampled aliquots of my condensed cultures until I had at least 20 living larvae on a Sedgewick rafter counting slide. In some sampling events, cups contained fewer than 20 live larvae, so I sampled the maximum number or larvae possible. All dead larvae in the aliquots

were counted for mortality ratios, and then discarded. The remaining living larvae (~20) on the slide were fixed in 4% formaldehyde solution for 24 hours, then stored in 70% ethanol in a -80°C freezer. In the following months, fixed samples were photographed on a Leica M125 Stereoscope, measured for shell length using ImageJ software, and identified to developmental stage by the presence or absence of a visible eye spot. Culturing continued until culture cups reached 70% competence, 95% mortality, or the end of the larval supply, with treatment cups lasting up to 17 days post larval release.

Analysis

I analyzed larval growth by plotting the average lengths of larval samples (n=2-44) through time in each culture cup, starting from a common baseline sample (day 0) from before larvae were distributed into experimental treatments. Using these average lengths, I ran linear regressions of larval length over time for each cup with a fixed intercept equal to average starting size (156µm), establishing daily growth rate in each treatment culture. I ran a Generalized Linear Model analysis with all water quality variables (mean values of temperature, salinity, pH, pCO_2, and aragonite saturation state for each culture cup) as continuous predictors and daily larval growth rate as the response variable. While I also obtained values of dissolved inorganic carbon (DIC) for each treatment cup, a correlation analysis showed very high collinearity between DIC and salinity (Supp Fig 1), so I did not use DIC as a predictor variable in models. Because temperature and salinity play a large role in determining gas solubility, there was a degree of covariation between carbonate chemistry variables with both other manipulated variables, particularly with salinity. pH was the least colinear of the carbonate

variables, so was therefore used as the default carbonate chemistry metric to be represented in figures and analyses. pH was also a measured variable in this experiment, whereas pCO_2 and Ω Ar were calculated in CO2SYS, so pH represents the most independent acidification variable in these analyses. I compared models using Akaike's Information Criterion (AIC) values, Bayesian Information Criterion (BIC) values, predictor significance, and adjusted R^2 values to find the optimal model fit (Supp Table 2).

To assess suitability of my treatment conditions as larval habitat, I considered cups in which 25% or more of sampled larvae reached the late pediveliger stage (displaying visible eyespots) as "suitable" treatments for larval survival. Presence of pediveligers suggests larvae are competent to settle, and therefore are able to live through larval life in the given treatment. I chose this 25% threshold to filter out any potential false positives from cross contamination of eyed larvae from pipettes or sieves during sampling. I used the treatment values of temperature, salinity, pH, pCO_2, and aragonite saturation state as continuous predictors to create a multiple logistic regression model for habitat suitability of treatments. I used AIC, BIC, predictor significance, and pseudo R^2 comparisons to select the best-fit model for these data (Supp Table 3).

Predicting Impacts in the Salish Sea

Having established specific effects of environmental parameters on growth rate and habitat suitability for larvae in the region, I used measured values of those parameters from two specific bays where Olympia oyster populations are found to analyze larval growth and larval habitat suitability in present-day conditions in the context of the broader environmental

tolerance range of the species. Then, I used projected present-day and future environmental conditions in the region to estimate *in situ* changes in growth and PLD in future oceanic conditions.

To examine larval tolerance to conditions in the natural environment, I focused on two particular state-operated restoration sites in the Salish Sea that we know contain breeding adults of the species: Fidalgo Bay and Liberty Bay, Washington (Blake & Bradbury 2012; Wasson et al. 2016). I used environmental data in Fidalgo Bay summarized in McIntyre et al. (in revision), and Cordoba and Arellano (unpublished data); both studies measured water quality variables throughout the water column in sampling efforts during mid-July of two separate summers. I obtained data from Liberty Bay from the Western Washington University SEA Discovery Center's long-term monitoring project, which measured water quality parameters from surface to depth twice weekly from 2017 – 2019, and averaged values from July 5 to Aug 23 (estimated peak larval season, Pritchard et al. 2015) during each year. With these two samples from Fidalgo Bay, and three from Liberty Bay, I project PLD and suitability of habitat for Olympia oyster larvae in realistic conditions in the Salish Sea.

To analyze near-future changes in the larval phase, I used data from the Pacific Northwest National Laboratory's Salish Sea Model (Khangaonkar et al. 2019, 2018), a hydrodynamic and water quality model of the Salish Sea, including a baseline condition in the year 2014, and a future projected oceanographic condition for the year 2095 modeled under an RCP 8.5 high CO_2 emissions scenario. Each model includes roughly 16,000 nodes throughout the larger Salish Sea region with values at 10 sigma layers between surface and bottom at each node. I first selected nodes in the regions of each of the 19 restoration sites in Washington

State that were between 0 and 20m deep (n=8-46 per site). Then, I averaged hourly values for relevant water quality parameters at each site between July 5 - August 23 during each year. Because this model utilizes a smoothing factor for the entire Salish Sea, environmental parameters in shallow areas are biased toward deeper water values in this model; as such, environmental values in restoration site bays are skewed, with temperature being especially underestimated. Because these values are underestimated, I use these data as an indication of trends between 2014 and 2095, but not as absolute numbers. Using my predictive growth rate model, I modeled PLD from release size of 156µm to competence size of 260µm in each of Washington State's active Olympia oyster restoration sites in the year 2014 and 2095. Though published estimates of competence size for Olympia oysters vary (Brink 2001; Hori 1933; Loosanoff et al. 1966), I chose 260µm as the a beginning competence size as this was the size at which I began seeing frequent eye spots in my experimental cultures (Fig 3) and is consistent with previous stage classifications from our lab (McIntyre et al., in revision). Due to the underestimated temperature values in the Salish Sea Model, I did not use these data to predict larval habitat suitability, as all points in 2014 would have been outside of the larval habitat suitability logistic regression curve.

Results

Treatment Values

Treatments in this experiment spanned wide ranges of each manipulated variable (13.05 – 29.65°C, 12.93 – 39.90 PSU, and 7.59 – 8.08 pH) (Fig 2, Supp Fig 2-3). Over the course of the experiment, treatment conditions varied due to biological factors, water changing error, and an unexpected decrease in inflow velocity later in the experiment (Supp Fig 2). The average standard deviation of conditions in culture cups over the duration of the experiment was 0.82°C temperature, 0.57PSU salinity, and 0.038 pH units. There was much higher variation over time in pH conditions than in temperature or salinity, and thus, pH values between treatments overlapped much more than did temperature or salinity (Supp Fig 2, 3). Still, most treatments remained distinct in their suites of conditions over the course of the experiment (Fig 2).

Larval Growth

Larvae in this experiment grew from their release sizes (135-175µm, averaging 156µm) to past 350µm and even larger as some larvae began settling in culture cups. Larvae became competent as early as day 5 in some treatments (Fig 3a). Not all cups reached competence, so I used 260µm as a standard competence size for modeling because this was the size above which most individuals were competent and most cultures contained 25% or more competent larvae (Fig 3a, 3b), and is consistent with size classifications from previous work in Dr. Arellano's Lab (McIntrye et al. in revision).

Daily larval growth rate varied greatly between my 50 environmental treatments from almost no growth (0.28µm/day) to 21.35µm/day, with the three fastest growth rates in cups G5, G4, and H5, all with mean temperatures all at approximately 26.5°C, mean salinities at 30, 33, and 36 PSU, and at a wide range of pH value, averaging 7.91, 7.75, and 7.66 (Fig 4, Supp Table 1). Indeed, results from my GLM model analysis showed that temperature and salinity greatly influence daily growth rate, but larvae did not respond to acidification at this scale (Supp Fig 4). No metric of acidification (total scale pH, pCO_2, aragonite saturation) improved the fit of the model individually or combined. As such, Fig 4-7 display treatments in cartesian coordinates of temperature and salinity only, even though each treatment cup does have a unique pH value (Fig 2, Supp Table 1). The final GLM model uses temperature, salinity, and a temperature*salinity interaction term to predict growth rate, explaining 71% of growth rate variance in experimental treatments (Table 1, Supp Table 2). Salinity in the GLM is used as a quadratic function wherein growth peaks at salinities slightly above 30PSU (Supp Fig 4).

A gridded bivariate interpolation (Fig 5a) shows the nonlinear best fit of growth between my experimental values, while Fig 5b shows the projected growth rate using my GLM. Absolute difference in real vs. model predicted growth rate peaks at cups G5, G4, and H5, the cups with highest growth, where the model underestimates predicted growth rates in these treatments compared to actual growth rates observed during the experiment. I also observed a decrease in growth rate at the highest temperature values that my model failed to predict (Fig 4, 5a, & 5b). However, as larvae in the Salish Sea are unlikely to experience these high temperatures in current or near-future scenarios, this model's high-temperature limitations are not particularly detrimental to this analysis.

Larval Habitat Suitability

Of the 50 environmental treatments, 16 were considered "suitable larval habitats" with 25% or more larvae surviving to competency (Fig 4). These 16 suitable habitat treatments had salinities centered around 30PSU, with more salinity treatments being suitable as temperatures increased (Figure 4). I used a multiple logistic regression to model habitat suitability across the environmental treatment cups. My final model uses temperature as a linear function and salinity as a quadratic function to predict larval habitat suitability (Table 2, Supp Table 3, Supp Fig 5). Again, no metric of ocean acidification (pH, pCO_2, or aragonite saturation) significantly predicted habitat suitability or improved the AIC of models at this scale (Supp Table 3).

Using this model, I correctly predicted habitat suitability in 48/50 experimental treatments, exemplifying the fit of this model to observed treatment responses (Fig 6a). I then predicted habitat suitability in crossed temperatures 11-30°C and salinities 9-39PSU, outlining the bivariate condition thresholds that describe suitable habitats for larval survival (Fig 6b).

Predicting Impacts in the Salish Sea

Measured temperature and salinity values in two Salish Sea oyster restoration sites (Liberty Bay and Fidalgo Bay) between summers 2014 and 2019 averaged 16.44 – 17.36°C, and 27.7 – 29.58 PSU, yielding projected PLDs averaging approximately 2.5 weeks (18 ± 0.6 days). The likelihood of suitable larval habitats in these sites ranged from 26.6% – 49.9% (Supp Table 4, Fig 7 black diamonds).

According to the Salish Sea Model, mean temperature and salinity in the 19 Washington State Olympia oyster restoration sites were 12.73 ± 1.31°C and 28.59 ± 1.44PSU in 2014, and 15.92 ± 1.29°C and 27.75 ± 1.09PSU in 2095 (Table 3, Fig 7). Using my larval growth GLM, predicted PLD decreased for larvae in every site between 2014 and 2095, ranging from a decrease of 3.4 days to 36.6 days (Figure 8, Table 3). Mean PLD among all sites decreased from 34.12 days in 2014 to 20.03 days in 2095.

Discussion

Climate stress and larval performance

Results of this experiment indicate that larvae of *O. lurida* will be robust to most major direct impacts of climate change. Larvae in this experiment actually performed better (faster developmental rate, increased tolerance to local habitats) in conditions representative of future environments in the Salish Sea in the next century and beyond. While the treatment conditions were somewhat variable throughout the course of the experiment, this variation was well within the range of daily variation larvae can experience in the natural environments (Mcintyre et al., in revision). I believe considering the number of treatments and the range of each variable, the variation experienced does not negate the patterns displayed using averaged environmental treatment cup values.

Salinity had a major impact on larval growth, but this impact was only strongly negative at levels that are unlikely to reflect averages in the Salish Sea in the present or near future (under ~21 PSU). Salinity influenced both larval growth rate and larval habitat suitability in a quadratic pattern with performance peaks at salinities around 30-33PSU, salinities which are regularly found in coastal environments where *O. lurida* live. No cultures were suitable for larval survival at salinities below 21PSU, but habitats were suitable for larvae in a wider range of salinities as temperatures increased (Figure 4). This pattern is consistent with temperature and salinity interactions in a similar model of *Crassostrea gigas* larvae (Hofmann et al. 2004) wherein larvae could withstand wider ranges of salinity at warmer temperatures. Because low salinity, low temperature water is rare in coastal environments during Olympia oyster spawning season in the Salish Sea, larvae of Olympia oysters are not likely to be adapted to withstand

such conditions. Low salinity in the water column would generally be surface water at higher temperatures, so larvae might be better adapted to these conditions as reflected in my larval habitat suitability model (Figure 6).

Larvae were resistant to all metrics of ocean acidification in this experiment including low pH, high pCO_2, and aragonite undersaturation. This finding is consistent with other studies using this species; Waldbusser et al. (2016) found no negative response of *O. lurida* larvae to acidic conditions, in contrast to major deformation in early shell building in *Crassostrea gigas* (Waldbusser et al. 2016). Hettinger et al. (2013a) found that *O. lurida* larvae had slight negative response to acidification, but this response was offset by high food availability, specifically at 100,000 cells/ml *I. galbana,* the level at which I fed larvae in this experiment (Hettinger et al. 2013). This resistance could be due to the fact that Olympia oysters brood their larvae (Lucey et al. 2015); a similar brooding oyster in the *Ostrea* genus showed resilience to pCO_2 that was largely attributed to adaptation during periods of sustained hypercapnia in the brood that exceeded near-future projections in acidifying oceans, and the fact that they are released into the water column as veligers which are most robust than earlier stages (Cole et al. 2016). It is possible, however, that due to the wide ranges of temperature and salinity in treatment cups, effects of acidification in this experiment simply went undetected compared to the strong signal of the other variables. The range of acidification treatment averages in this experiment was 7.59 – 8.08 pH, or 362.12 – 1205.3 pCO_2, which may be relatively lower than the ranges of salinity and temperature, though similar work has shown strong physiological responses to acidification within this magnitude in other bivalve species (Barton et al. 2012; Miller et al. 2009; Talmage & Gobler 2011) .

Temperature had a strong positive relationship with growth rate, as is to be expected with marine larvae and most ectotherms. However, the temperature that yielded highest growth rate in this experiment was considerably higher than I expected. Larval growth rate in this experiment peaked at around 26.5°C, with slower growth at temperatures above and below this peak. This pattern suggests that *O. lurida* from the Salish Sea can tolerate a degree of considerable warming before hotter temperatures reduce their growth rates, likely compromising protein functions in development (Byrne 2011). However, because my growth model only predicts a positive linear relationship with temperature, it should not be applied for temperatures above 30°C. Temperature was also positively correlated with habitat suitability in this experiment. Treatment conditions were more likely to be suitable for larval growth and survival at higher temperatures, and a wider range of salinity treatments were suitable as temperature increased. Interestingly, larvae displayed little growth and low tolerance to habitat conditions at temperatures reflective of averages in the greater Salish Sea, as suggested by the deep-region-biased Salish Sea Model values. This pattern suggests that in order to maintain successful populations, Olympia oysters are likely either limited to shallow bays where temperature is higher, or that larvae use behaviors to stay in warmer waters throughout larval life. My results are consistent with previous studies reviewed in Strathmann (1987) finding that *O. lurida* larvae at low temperatures (14-16°C) show little growth and do not live past 20 days, larvae at 16-18.5°C might grow and survive, but largely do not metamorphose (Davis 1949), and larvae in temperatures around 24° can settle in as little as 7 days (Loosanoff & Davis 1963).

Overall, this experiment identified clear patterns of environmental optima for Olympia oyster larvae. Larvae very clearly grew faster and were more likely to tolerate habitats in

warmer treatments at salinities around 30PSU, with no effects of acidification on larval performance. Though baseline mortality in this experiment was noticeably higher than in similar studies in our lab (potentially due to poorer larval condition at the end of the spawn season), I am confident in the relative patterns of success in these treatments. Though this study is limited to the larval stage only and does not consider environmental bottlenecks of settlement or metamorphosis, when focusing on the larval stage alone, the outlook in near-future climate change scenarios is positive for this species.

Model validity in the Salish Sea

Between experiment findings and field projections in this study, I found larvae becoming competent as early as day 5 (in my fastest growing experimental treatment) and as late as day 58 (in my longest projected PLD from the Salish Sea Hydrodynamic Model). This PLD range aligns well with the range in a recent review of the species, which lists PLD from 1-8 weeks (Pritchard et al. 2015).

Using measured environmental values in Fidalgo Bay from 2014 and 2017, I predict PLD at this site to be about 18 days (Supp table 4). This prediction is consistent with estimated PLD from recruitment measurements in the same bay in summer 2015, which measured 2 weeks between peak reproduction and peak larval settlement of the population (Hintz, unpublished data). The slightly shorter duration in 2015 may be explained by the presence of a marine heat wave in the Salish Sea and throughout the North American West Coast during the Olympia oyster spawning season of 2015. Projected PLDs were similar using environmental values from Liberty Bay from 2017 - 2019, which yielded PLDs from 16.9-18.5 days. One caveat of these data

is that all of these field parameters were measured during daylight hours only, so could be slightly overestimating temperature and underestimating salinity compared to 24-hour samples.

Knowledge of optimal larval conditions can inform restoration on both local and regional scales. For example, given the low larval habitat suitability of colder and less saline treatments in this experiment and the theoretical exponential increase in the likelihood of mortality throughout PLD, I suggest restoration efforts focused on warmer-water sites with salinities closer to 30PSU will yield increased settlement opportunities and population stability compared colder and/or less saline sites. At a larger scale, because of their high tolerance to acidification, Olympia oysters will be a more sustainable species for focused coast-wide oyster bed restoration efforts than now-common species such as Pacific oysters, that will likely not fare as well when the region continues to acidify.

Future anticipation of environmental change in the Salish Sea will help guide restoration efforts long term. The Salish Sea Model predicts that oyster restoration habitats in the Salish Sea will be approximately 3-4° warmer, and 1-2 units less saline in 2095 than they were in 2014 (Table 3, Figure 7). While I did not estimate future larval habitat suitability due to the underestimated environmental values in the Salish Sea Model, I used the Salish Sea Model data to analyze relative change in PLD in future oceans and consider implications for larval ecology. Additionally, while temperature and salinity values are underestimated in these nearshore sites, they are representative of the Salish Sea as a whole, so are well within the realm of possibility for larvae that disperse out of their shallow bays into deeper, colder water.

Projected PLDs in 2014 restoration site conditions showed considerable site-to-site variation from 21-58 days. In 2095 conditions, PLDs at all sites decrease, with average across-site PLD decreasing by 41% (Fig 8, Table 3). This dramatic decrease will influence both the community structures of the region, as well as population dynamics of the species. Larvae make up a substantial portion of planktonic communities (Kulikova et al. 2000), so if these patterns are consistent in other species, this PLD decrease could represent a fundamental paradigm shift in planktonic community composition. Decreased presence of meroplankton might have important implications for food webs or ecosystem interactions and should be a key consideration in future coastal dynamics models for fisheries and ecology. Further, this decreased PLD may limit future dispersal and metapopulation connectivity for Olympia oyster populations in the Salish Sea, as these fragmented populations likely depend on larval transport to sustain genetic diversity. Because shortened PLDs will limit the timeframe during which *O. lurida* larvae can access ocean currents, patterns of future dispersal will be subject to change as effects of climate change increase.

Ostrea lurida, climate, and ecological theory

While results from this experiment can inform conservation efforts in the Salish Sea, they can also explain much of the ecology and current distribution of the species. The wide range of environmental tolerance I observed in *O. lurida* larvae is consistent with the species' historical and current distribution over a large geographic range from British Columbia to Baja California (Pritchard et al. 2015; Silliman 2019; Wasson et al. 2016). As this range is characterized in part by large sections of local acidification from upwelling in the Salish Sea and

the California Coast (Chan et al. 2017), *O. lurida's* resistance to pH stress likely facilitates its distribution across these regions. This particular larval resistance to acidification is in stark contrast with other species such as *Crassostrea virginica* and *Crassostrea gigas,* that have both exhibited negative responses to acidification within this acidification range (Barton et al. 2012; Miller et al. 2009), and are not native to such chemically variable regions, highlighting the link between species distribution and evolutionary history for benthic and sessile marine organisms. Success in a wide range of temperatures allows *O. lurida* to inhabit this large latitudinal range, from temperate conditions in Washington and British Columbia, to subtropical seas in Baja California. The environmental conditions at Liberty Bay and Fidalgo Bay, two active Olympia oyster restoration sites in the Salish Sea in five samples between 2014 and 2019 all fell below 50% likelihood in my logistic model to predict larval habitat suitability (Fig 7). Considering this, I suggest that the *O. lurida* populations in Washington State and British Columbia likely live at an environment-driven range edge for the species, and one that may break down as ocean temperatures continue to rise. *Ostrea lurida* larvae are sensitive to low salinities, but it is possible that they rarely encounter these values in the natural environment or use behaviors to avoid them. Interestingly, these findings suggest that *O. lurida* in the Salish Sea are operating far below their environmental optimum, based on both the Salish Sea Model (which likely underestimates temperature) and the field site conditions collected in known Olympia oyster habitats in Fidalgo Bay and Liberty Bay (Fig 7). This begs the question of why their range extends to regions like the Salish Sea in which they seem poorly adapted, and how these range edges will fare in future ocean conditions.

It has been a long-standing hypothesis in larval ecology that the evolution of pelagic larval life histories developed as a mechanism for dispersal and genetic connectivity for sessile or otherwise mobility-limited marine invertebrates (Scheltema 1971; Swearer et al. 2002). According to this theory, the relatively long PLD of Olympia oysters in the Salish Sea might be beneficial for dispersal and connectivity of populations and might even be what allowed them to settle in suitable habitats that are patchily distributed throughout the region. This ability to disperse among the broader metapopulations in distant suitable habitat regions might aid in their persistence, despite the suboptimal environmental conditions in the region.

However, organisms with fully pelagic life histories and those with unlimited adult mobility still often have a pelagic larval stage, negating the necessity of a dispersal function for the evolution of pelagic marine larvae. Additionally, prominent morphological features on some types of larvae promote increased drag, not drift in the water column (Emlet 1983), and measured dispersal of invertebrate populations is often less than the distance of passive transport (Shanks 2009; Shanks et al. 2003), suggesting that larval phases are not always evolutionarily adapted for the longest possible dispersal. Pechenik (1999) suggests that the pelagic larval stage might indeed be an evolutionary liability and that short PLD and small dispersal ranges are beneficial to populations (Pechenik 1999). Because the presence of reproductive adults in an area implies the presence of suitable habitat for a species, short PLD and dispersal distance would increase chances that larvae would retain access to such suitable habitat. Shortened PLDs might also decrease wastage of populations, as the larval phase is disproportionately vulnerable and experiences exponential decreases in survivorship over time (O'Connor et al. 2007). Considering this, Olympia oyster larvae in the Salish Sea will likely

benefit from some level of near-future climate change. Populations will see increased larval growth rate and increased access to suitable larval habitats but may sacrifice connectivity between metapopulations.

Crassostrea virginica populations on the U.S. East Coast show compromised population stability in higher latitudes due to changes in growth, reproduction, and post-settlement mortality at colder temperatures (Powell et al. 1994). Related research using the same study populations found decreases in PLD in lower latitudes and higher self-recruitment at higher temperatures, adding to these population structure differences (Dekshenieks et al. 2000, 1993). While here, I focus only on the larval phase, I hypothesize that a similar latitudinal population stability gradient for *O. lurida* may exist. By having access to more suitable habitat and having higher probability of self-recruitment due to shortened PLDs at higher temperatures, *O. lurida* populations might be less vulnerable to population crashes at lower latitudes. Similarly, ocean warming from climate change may increase population stability of *O. lurida* in the Salish Sea over time and allow for recruitment in even higher latitudes as effects of climate change increase. Further study on reproduction and environment-dependent dispersal potential could test this hypothesis.

Tables and Figures

Table 1: Model summary of Generalized Linear Model for larval growth, using temperature and salinity as predictor variables for larval growth rate

Growth Rate ~ Salinity + Salinity^2 + Temperature + Salinity*Temperature				
Parameter	Value	SE	t	p
(Intercept)	-13.09	6.38	-2.05	< 0.05
Salinity	1.12	0.37	2.99	< 0.01
Salinity^2	-0.03	0.01	-4.44	<< 0.01
Temperature	-0.22	0.23	-0.95	0.35
Temp*Sal	0.03	0.01	3.37	< 0.01
Residual standard error: 2.608 on 45 degrees of freedom				
Multiple R-squared: 0.7382		F-statistic: 31.72 on 4 and 45 DF		
Adjusted R-squared: 0.7149		p-value: 1.414e-12		

Table 2: Model summary of multiple logistic regression model of treatment habitat suitability for Olympia oyster larvae using temperate and salinity as predictor variables for suitability. Pseudo R^2 was calculated using McFadden's Adjusted R^2 formula.

Suitability ~ Salinity + Salinity^2 + Temperature				
Parameter	Value	SE	z	p
(Intercept)	-122.61	46.51	-2.64	< 0.01
Salinity	7.31	2.80	2.61	< 0.01
Salinity^2	-0.12	0.05	-2.62	< 0.01
Temperature	0.82	0.33	2.50	< 0.05
Null deviance: 62.687 on 49 degrees of freedom Residual deviance: 12.553 on 46 degrees of freedom		AIC: 20.553 Number of Fisher Scoring iterations: 9		
Pseudo R^2 : 0.67		R^2 p-value: 7.479894e-11		

Table 3: Mean temperature and salinity from the Salish Sea Hydrodynamic Model from July 5-August 23 2014 and 2095 in the 19 state-managed Olympia oyster restoration sites in Washington State with average model-predicted PLD in each site for each year. Last column shows change in projected PLD in each site for each year. Last column shows change in projected PLD between 2014 and 2095 conditions.

	2014			2095			**Δ**
Site	Temperature	Salinity	PLD	Temperature	Salinity	PLD	PLD
Bellingham Bay	13.64	26.53	25.64	16.47	25.89	18.9	-6.74
Budd Inlet	15.04	25.23	22.19	16.5	26.02	18.78	-3.4
Discovery Bay	10.93	30.9	58.49	15	28.74	21.84	-36.65
Drayton Harbor	11.34	28.76	40.64	14.2	28.26	24.07	-16.57
Dyes Inlet	13.47	28.83	27.12	16.91	28.45	17.59	-9.54
Fidalgo Bay	12.64	28	30.29	16.09	26.44	19.39	-10.9
Henderson Bay	13.61	28.58	26.39	16.15	28.07	19.02	-7.37
Kilisut Harbor	10.94	30.55	54.93	14.4	28.96	23.75	-31.17
Liberty Bay	12.5	28.75	31.9	15.92	28.5	19.55	-12.36
Padilla Bay	12.61	27.73	30.25	16.47	26.09	18.82	-11.44
Port Gamble Bay	12.27	30.16	36.48	15.24	29.04	21.3	-15.19
Port Orchard Pass	13.05	28.83	29.07	15.96	28.33	19.43	-9.64
Quilcene Bay	10.93	29.81	49.96	13.69	28.86	26.24	-23.72
Samish Bay	13.13	27.94	27.94	17.48	26.19	17.12	-10.82
Sequim Bay	11.21	30.54	50.29	15.67	28.02	20.04	-30.25
Similk Bay	12.11	26.81	32.29	14.65	27.13	22.55	-9.73
Sinclair Inlet	13.41	28.56	27.17	16.32	28.4	18.69	-8.48
Squaxin Island	13.54	28.58	26.65	16.01	28.12	19.33	-7.32
Union River	15.42	28.13	20.63	19.43	27.76	14.16	-6.47

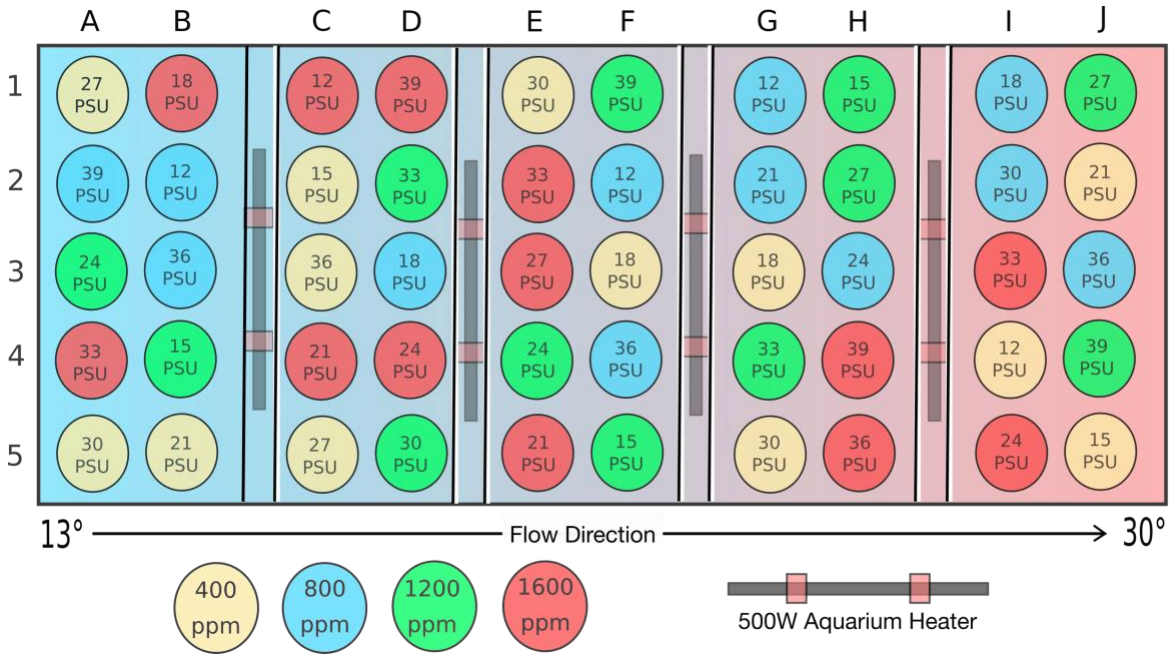

Figure 1: Growth experiment scheme. The culturing tank had inflow on the left end, direction flow towards the right, and four 500W digital submersible aquarium heaters heating the water as it flowed into each new chamber. Each heat chamber contains 10 culture cups, each randomly assigned a CO_2 value of 400, 800, 1200, or 1600 ppm, and a salinity value from 12-39PSU in units of three. All four CO_2 values and ten salinity values are present within each 10-cup temperature group.

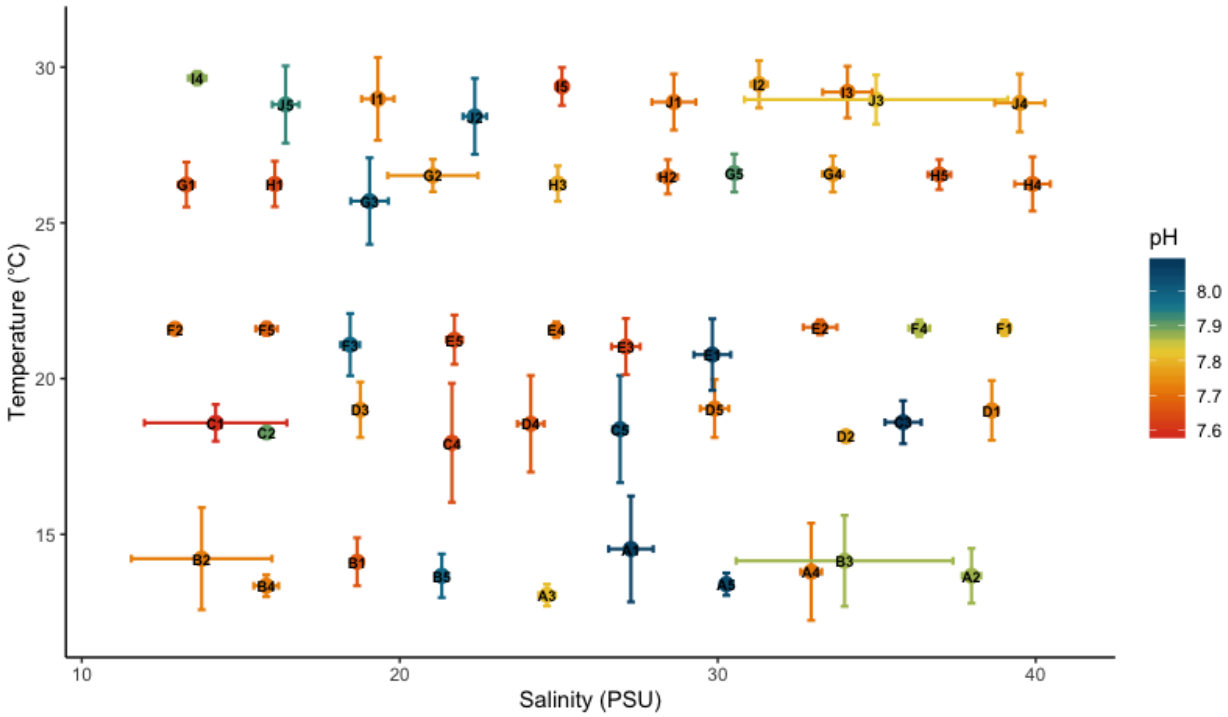

Figure 2: Average treatment values of culture cups in the experiment. X and Y axes represent mean salinity and temperature, color represents average pH. Error bars represent standard deviation of temperature and salinity for the duration of the cup's inclusion in the experiment (3-17 days). Average standard deviation of salinity was ±0.59 PSU, temperature was ±0.83°C, and pH was ±0.03 pH units.

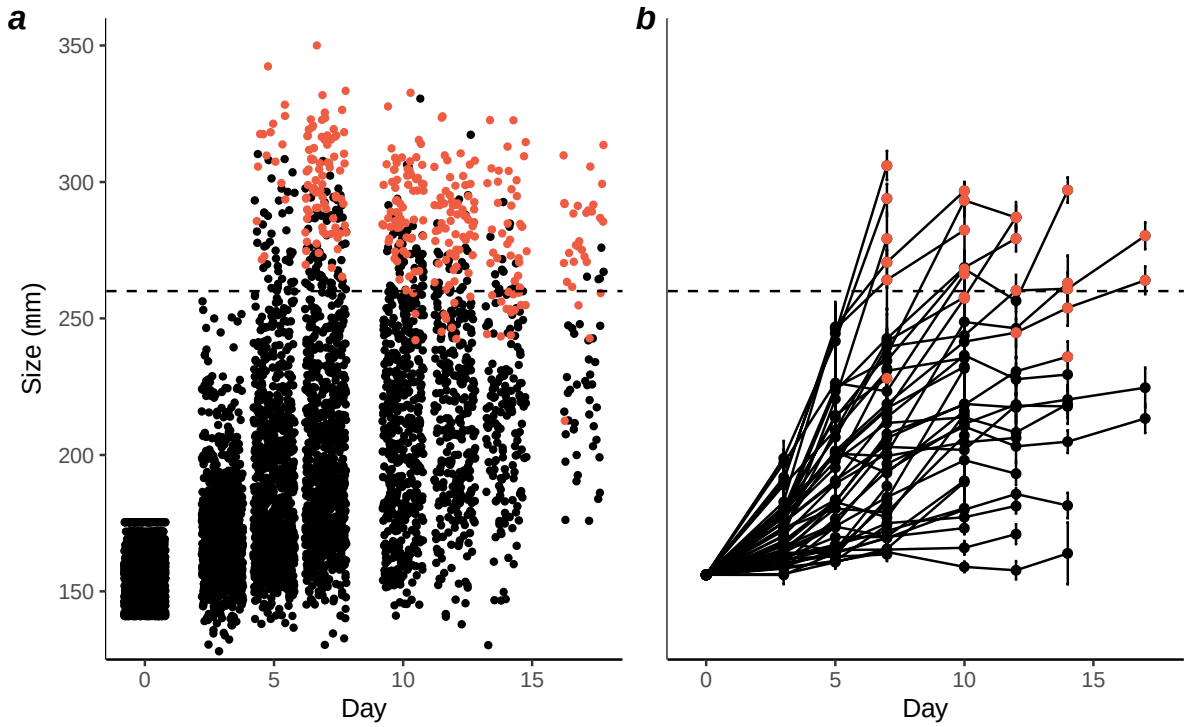

Figure 3: Size values through time of all larvae across experimental treatments. a) larval sizes in all treatment cups where black dots represent non-competent larvae (lacking a visible eyespot) and red dots represent competent larvae. b) average sizes with error bars ±SD for larval treatment cups. Red dots represent samples where over 25% or larvae sampled were visibly competent. In both plots, the horizontal line at 260µm represents the size at which I considered larvae late-stage veligers.

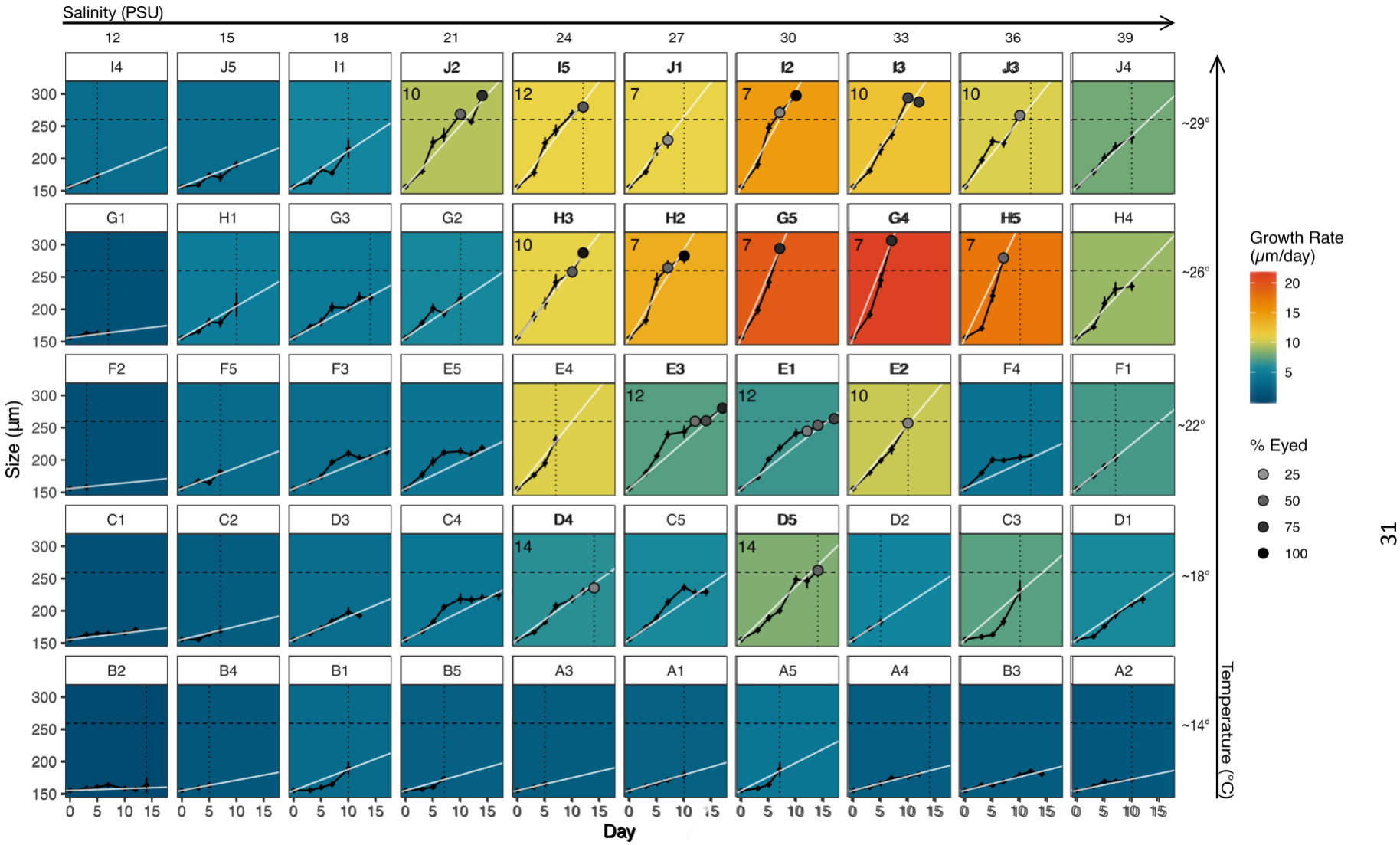

Figure 4: Growth of oyster larvae in 50 climate treatments arranged by target salinity (left-right) and target temperature (bottom-top). Black lines are lengths of larval shells (n=3-44), white lines are linear regressions, showing average growth/day. Horizontal dotted line represents late-stage larva size (260µm). Filled in circles represent proportion of sampled larvae with visible eyespots at all samples >25%. Vertical dotted lines indicate >95% mortality. Panel color represents growth rate (µm/day). Numbers denote theoretical first sampling of >25% eyed larvae in each cup.

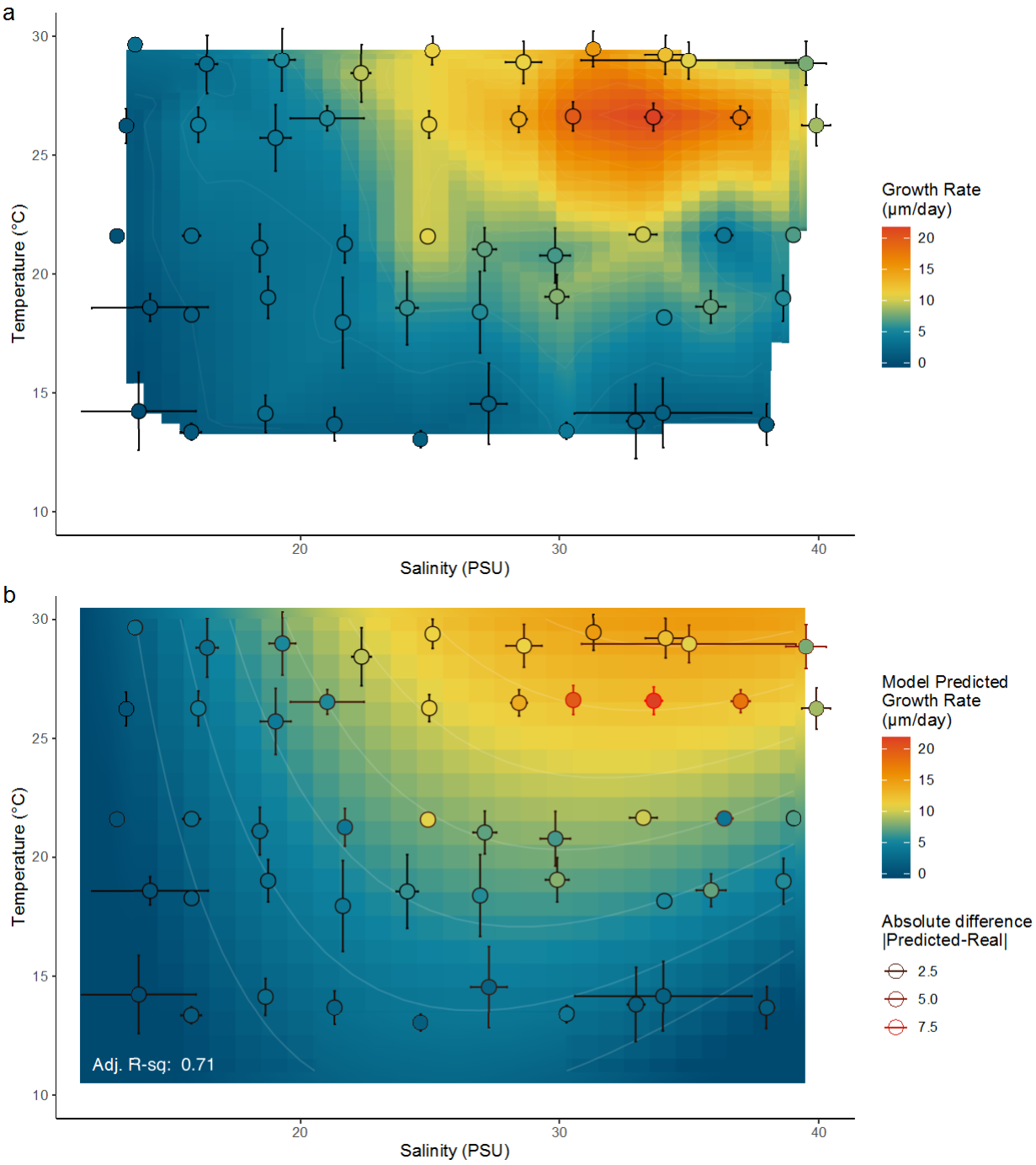

Figure 5 a) Gridded Bivariate Interpolation of growth rate between experimental temperature and salinity coordinates, overlaid with real values of growth rate in experimental treatment points. b) Predicted growth rate using Generalized Linear Model function at every salinity (9-39PSU) and temperature (11-30°C) combination with experimental treatments overlaid. Color inside points represents real growth rate in given experimental treatment, while color of the panel represents modeled growth rate. Outline colors of points and error bars represent the absolute difference between real and predicted growth, where red outlined points are more poorly predicted by the model.

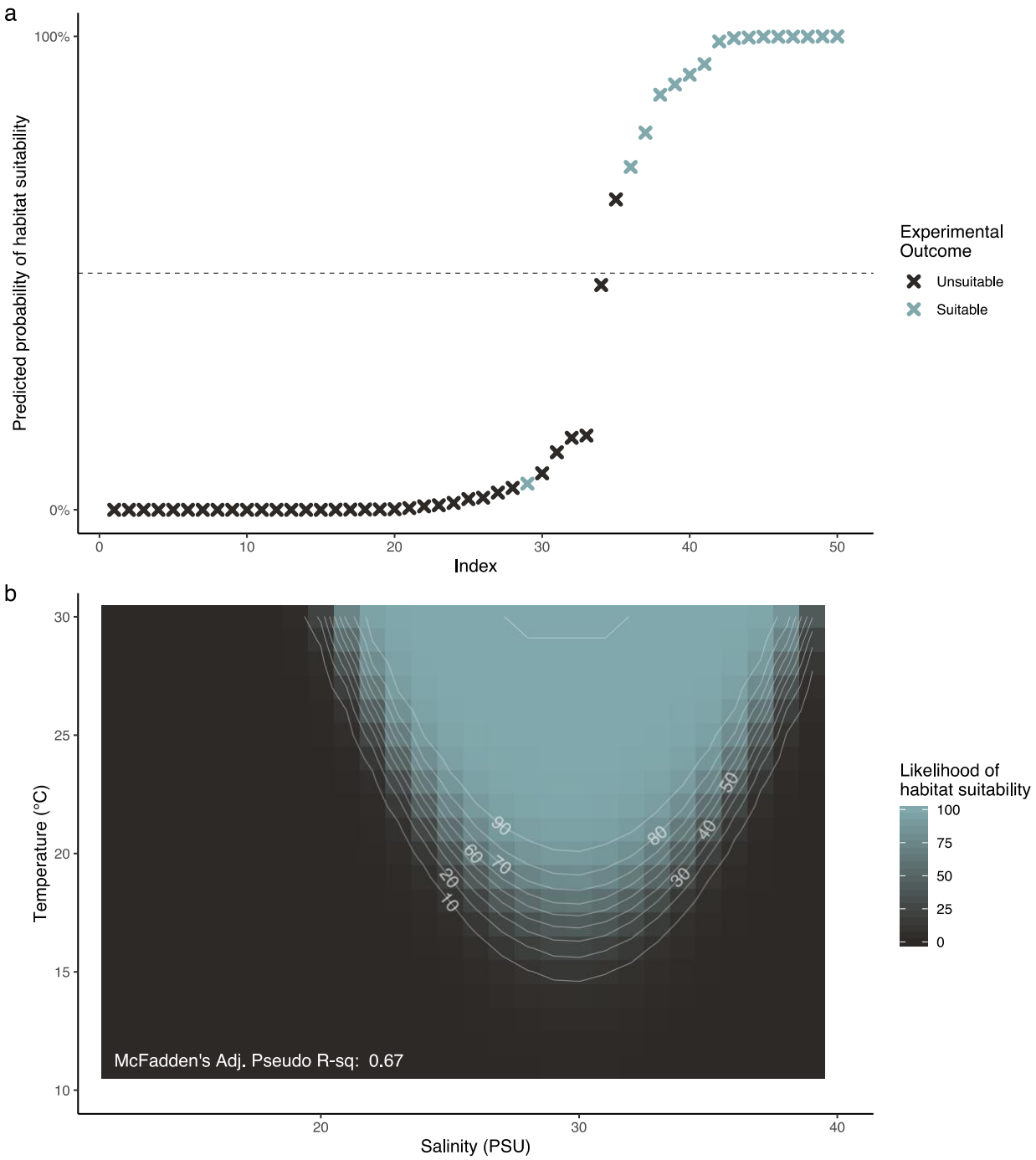

Figure 6 : Habitat suitability likelihood of experimental treatments for Olympia oyster larvae. a) Predicted habitat suitability in 50 environmental treatments. Treatments above the horizontal line are predicted as survivable. Color represents actual suitability in experimental treatments. b) GLM-predicted likelihood of suitability across salinity (9-39PSU) and temperature (11-30°C). Color represents percent likelihood of 25% or more larvae in given environmental conditions growing to competency.

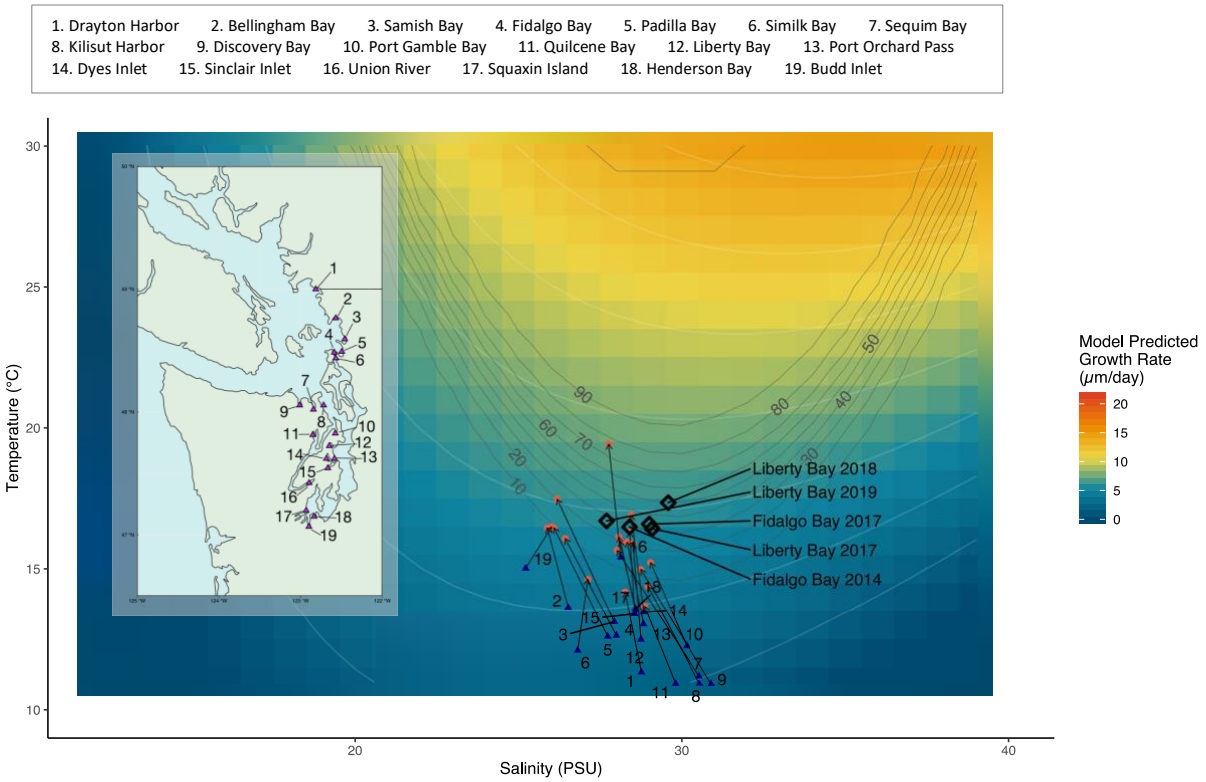

Figure 7: Predicted growth rate using Generalized Linear Model larval growth function with averaged temperature and salinity coordinates of 19 state-managed Olympia oyster restoration sites from July 5 – August 23 2014 (blue triangles) and 2095 (red circles) calculated from values in the Salish Sea Hydrodynamic Model. Black diamonds represent average values measured in two bays of restoration focus. White numbered contour lines represent likelihood that treatment will be suitable larval habitat. Inset shows site locations in the Salish Sea.

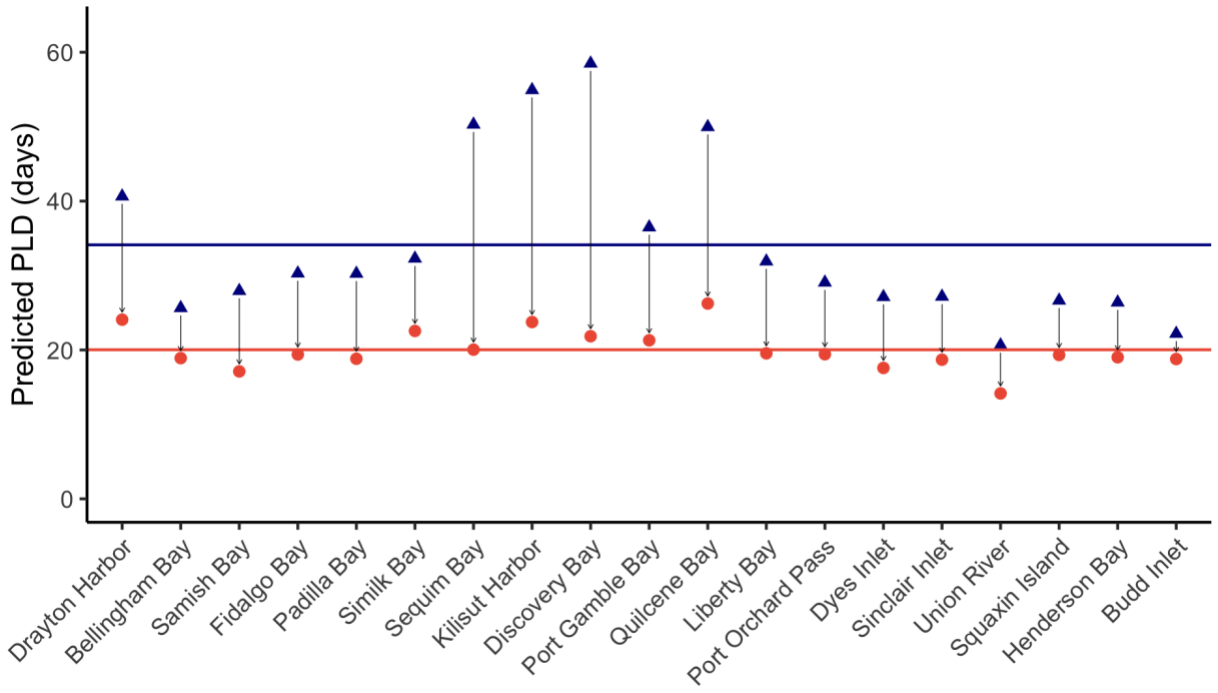

Figure 8 : Predicted pelagic larval duration of oysters released in each of the 19 state-managed restoration sites for the species in Washington State ordered North-South in the Salish Sea. Points represent time for simulated larvae to grow from release size(156µm) to competence size (260µm) in averaged values temperature and salinity values from hourly timepoints from July 4 – August 23, 2014 (blue triangles) and 2095 (red circles). Horizontal lines represent average duration in PLD over all sites in each year. Vertical arrows show change in projected PLD from 2014 to 2095.

References

Barros, P., Sobral, P., Range, P., Chícharo, L., & Matias, D. (2013). Effects of sea-water acidification on fertilization and larval development of the oyster *Crassostrea gigas* . *Journal of Experimental Marine Biology and Ecology*, *440*, 200–206. https://doi.org/10.1016/j.jembe.2012.12.014

Barton, A., Hales, B., Waldbusser, G. G., Langdon, C., & Feelyd, R. A. (2012). The Pacific oyster, Crassostrea gigas, shows negative correlation to naturally elevated carbon dioxide levels: Implications for near-term ocean acidification effects. *Limnology and Oceanography*, *57*(3), 698–710. https://doi.org/10.4319/lo.2012.57.3.0698

Barton, A., Waldbusser, G. G., Feely, R. A., Weisberg, S. B., Newton, J. A., Hales, B., … McLaughlin, K. (2015). Impacts of coastal acidification on the Pacific Northwest shellfish industry and adaptation strategies implemented in response. *Oceanography*, *28*(2), 146–159. https://doi.org/10.5670/oceanog.2015.38

Beadle, B. Y. L. C. (1931). The Effect of Salinity Changes on the Water Content and Respiration of Marine Invertebrates. *Journal of Experimental Biology*, *8*(3), 211–227.

Beck, M. W., Brumbaugh, R. D., Airoldi, L., Carranza, A., Coen, L. D., Crawford, C., … Guo, X. (2011). Oyster Reefs at Risk and Recommendations for Conservation, Restoration, and Management. *BioScience*, *61*(2), 107–116. https://doi.org/10.1525/bio.2011.61.2.5

Blake, B., & Bradbury, A. (2012). *Washington Department of Fish and Wildlife Plan for Rebuilding Olympia Oyster (Ostrea lurida) Populations in Puget Sound with a Historical and Contemporary Overview*.

Brink, L. A. (2001). Molluscs: Bivalvia. In *Identification Guide to Larval Marine Invertebrates ofthe Pacific Northwest* (pp. 129–149).

Byrne, M. (2011). Impact of ocean warming and ocean acidification on marine invertebrate life history stages: vulnerabilities and potential for persistence in a changing ocean. *Oceanography and Marine Biology: An Annual Review*, *49*, 1–42. https://doi.org/10.1016/j.marenvres.2011.10.00

Byrne, M., & Przeslawski, R. (2013). Multistressor impacts of warming and acidification of the ocean on marine invertebrates' life histories. *Integrative and Comparative Biology*, *53*(4), 582–596. https://doi.org/10.1093/icb/ict049

Chan, F., Barth, J. A., Blanchette, C. A., Byrne, R. H., Chavez, F., Cheriton, O., … Washburn, L. (2017). Persistent spatial structuring of coastal ocean acidification in the California Current System. *Scientific Reports*, *7*(1), 1–7. https://doi.org/10.1038/s41598-017-02777-y

Cole, V. J., Parker, L. M., O'Connor, S. J., O'Connor, W. A., Scanes, E., Byrne, M., & Ross, P. M. (2016). Effects of multiple climate change stressors: ocean acidification interacts with warming, hyposalinity, and low food supply on the larvae of the brooding flat oyster *Ostrea angasi* . *Marine Biology*, *163*(5), 1–17. https://doi.org/10.1007/s00227-016-2880-4

Davis, H. C. (1949). On cultivation of larvae of *Ostrea lurida*. *The Anatomical Record*, *105*, 111.

Dekshenieks, M. M., Hofmann, E. E., Klinck, J. M., & Powell, E. N. (2000). Quantifying the Effects of Environmental Change on an Oyster Population: A Modeling Study. *Estuaries*, *23*(5), 593–610. https://doi.org/10.2307/1352887

Dekshenieks, M. M., Hofmann, E. E., Powell, E. N., & Powell, E. N. (1993). Environmental Effects on the Growth and Development of Eastern Oyster, *Crassostrea virginica* (Gmelin , 1791), Larvae : A Modeling Study. *Journal of Shellfish Research*, *12*(2), 241–254.

Dickson, A., Sabine, C., & Christian, J. (Eds). (2007). Guide to Best Practices for Ocean CO2 Measurements. In *PICES Special Publication 3* (p. 191).

Doney, S. C., Fabry, V. J., Feely, R. a, & Kleypas, J. a. (2009). Ocean acidification: the other CO2 problem. *Annual Review of Marine Science*, *1*, 169–192. https://doi.org/10.1146/annurev.marine.010908.163834

Emlet, R. B. (1983). Locomotion, Drag, and the Rigid Skeleton of larval Echinoderms. *Biological Bulletin*, (164), 433–445.

Fabry, V. J., Seibel, B. A., Feely, R. A., Fabry, J. C. O., & Fabry, V. J. (2008). Impacts of ocean acidification on marine fauna and ecosystem processes. *ICE Journal of Marine Science*, (65), 414–432.

Feely, R. A., Orr, J., Fabry, V. J., Kleypas, J. A., Sabine, C. L., & Langdon, C. (2009). Present and future changes in seawater chemistry due to ocean acidification. *Geophysical Monograph Series*, *183*(Table 1), 175–188. https://doi.org/10.1029/2005GM000337

Gaines, S., & Roughgarden, J. (1985). Larval settlement rate: A leading determinant of structure in an ecological community of the marine intertidal zone. *Proceedings of the National Academy of Sciences*, *82*(11), 3707–3711. https://doi.org/10.1073/pnas.82.11.3707

Havenhand, J., Dupont, S., & Quinn, G. P. (2010). Part 2 : Experimental design of perturbation experiments, 4 Designing ocean acidifi cation experiments to maximise inference. *Guide to Best Practices for Ocean Acidification Research and Data Reporting*, (January), 67–80.

Hettinger, A., Sanford, E., Hill, T. M., Hosfelt, J. D., Russell, A. D., & Gaylord, B. (2013). The influence of food supply on the response of Olympia oyster larvae to ocean acidification. *Biogeosciences*, *10*(10), 6629–6638. https://doi.org/10.5194/bg-10-6629-2013

Hettinger, A., Sanford, E., Hill, T. M., Russell, A. D., Sato, K. N. S., Hoey, J., … Gaylord, B. (2012). Persistent carry-over effects of planktonic exposure to ocean acidification in the Olympia oyster. *Ecology*, *93*(12), 2758–2768. https://doi.org/10.1890/12-0567.1

Hofmann, E. E., Powell, E. N., Bochenek, E. A., & Klinck, J. M. (2004). A modelling study of the influence of environment and food supply on survival of *Crassostrea gigas* larvae. *ICES Journal of Marine Science*, *61*(4), 596–616. https://doi.org/10.1016/j.icesjms.2004.03.029

Hori, J. (1933). On the development of the Olympia oyster, *Ostrea lurida* Carpenter, Transplanted from United States to Japan. *Bulletin of the Japanese Society for the Science of Fish*, *1*(6), 269–276.

IPCC. (2019). Chapter 5: Changing ocean, marine ecosystems, and dependent communities. Intergovernmental Panel of Climate Change. *IPCC Special Report for the Ocean and*

Cryosphere in the Changing Climate, 1–198.

Khangaonkar, T., Nugraha, A., Xu, W., & Balaguru, K. (2019). Salish Sea Response to Global Climate Change, Sea Level Rise, and Future Nutrient Loads. *Journal of Geophysical Research: Oceans*, 2018JC014670. https://doi.org/10.1029/2018JC014670

Khangaonkar, T., Nugraha, A., Xu, W., Long, W., Bianucci, L., Ahmed, A., … Pelletier, G. (2018). Analysis of Hypoxia and Sensitivity to Nutrient Pollution in Salish Sea. *Journal of Geophysical Research: Oceans*, *123*(7), 4735–4761. https://doi.org/10.1029/2017JC013650

Ko, G. W. K., Chan, V. B. S., Dineshram, R., Choi, D. K. S., Li, A. J., Ziniu, Y., & Vengatesen, T. (2013). Larval and Post-Larval Stages of Pacific Oyster (Crassostrea gigas) Are Resistant to Elevated CO2. *PLoS ONE*, *8*(5), 1–12. https://doi.org/10.1371/journal.pone.0064147

Ko, G. W. K., Dineshram, R., Campanati, C., Chan, V. B. S., Havenhand, J., & Thiyagarajan, V. (2014). Interactive effects of ocean acidification, elevated temperature, and reduced salinity on early-life stages of the pacific oyster. *Environmental Science and Technology*, *48*(17), 10079–10088. https://doi.org/10.1021/es501611u

Kroeker, K. J., Kordas, R. L., Crim, R., Hendriks, I. E., Ramajo, L., Singh, G. S., … Gattuso, J. P. (2013). Impacts of ocean acidification on marine organisms: Quantifying sensitivities and interaction with warming. *Global Change Biology*, *19*(6), 1884–1896. https://doi.org/10.1111/gcb.12179

Kroeker, K. J., Kordas, R. L., Crim, R. N., & Singh, G. G. (2010). Meta-analysis reveals negative yet variable effects of ocean acidification on marine organisms. *Ecology Letters*, *13*(11), 1419–1434. https://doi.org/10.1111/j.1461-0248.2010.01518.x

Kulikova, V. A., Solokhina, E. V., & Samatov, A. D. (2000). Meroplankton of Avachinskii Inlet (Kamchatka). *Russian Journal of Marine Biology*, *26*(1), 1–7. https://doi.org/10.1007/BF02759486

Li, J., Jiang, Z., Zhang, J., Mao, Y., Bian, D., & Fang, J. (2014). The potential of ocean acidi fi cation on suppressing larval development in the Pacific oyster *Crassostrea gigas* and blood cockle *Arcain flata* Reeve *. *Chinese Journal of Oceanology and Limnology*, *32*(6), 1307–1313.

Long, W., & Khangaonkar, T. (2014). Approach for Simulating Acidification and the Carbon Cycle in the Salish Sea to Distinguish Regional Source Impacts. In *Washington Department of Ecology*.

Loosanoff, V. L., & Davis, H. C. (1963). Rearing of Bivalve Mollusks. *Advances in Marine Biology*, *1*, 1:136.

Loosanoff, V. L., Davis, H. C., & Chalney, P. E. (1966). Dimensions and Shapes of Larvae of Some Marine Bivalve Mollusks. *Malacologia*, *4*(2), 351–435. Retrieved from https://archive.org/details/cbarchive_48893_dimensionsandshapesoflarvaeofs1966/page/n35

Love, B. A., Olson, M. B., & Wuori, T. (2017). Technical Note: A minimally invasive experimental system for pCO2 manipulation in plankton cultures using passive gas exchange (atmospheric carbon control simulator). *Biogeosciences*, *14*(10), 2675–2684.

https://doi.org/10.5194/bg-14-2675-2017

Lucey, N. M., Lombardi, C., Demarchi, L., Schulze, A., Gambi, M. C., & Calosi, P. (2015). To brood or not to brood: Are marine invertebrates that protect their offspring more resilient to ocean acidification? *Scientific Reports*, *5*(June), 1–7. https://doi.org/10.1038/srep12009

Mcintyre, B. A., McPhee-Shaw, E. E., Hatch, M. B., & Arellano, S. M. (n.d.). Current speed affects the vertical distribution of Olympia oyster (*Ostrea lurida*) larvae in Fidalgo Bay, WA. *Estuaries and Coasts*.

Miller, A. W., Reynolds, A. C., Sobrino, C., & Riedel, G. F. (2009). Shellfish face uncertain future in high CO2 world: Influence of acidification on oyster larvae calcification and growth in estuaries. *PLoS ONE*, *4*(5). https://doi.org/10.1371/journal.pone.0005661

Millero, F. J., Graham, T. B., Huang, F., Bustos-Serrano, H., & Pierrot, D. (2006). Dissociation constants of carbonic acid in seawater as a function of salinity and temperature. *Marine Chemistry*, *100*(1–2), 80–94. https://doi.org/10.1016/J.MARCHEM.2005.12.001

Narita, D., Rehdanz, K., & Tol, R. S. J. (2012). Economic costs of ocean acidification: A look into the impacts on global shellfish production. *Climatic Change*, *113*(3–4), 1049–1063. https://doi.org/10.1007/s10584-011-0383-3

O'Connor, M. I., Bruno, J. F., Gaines, S. D., Halpern, B. S., Lester, S. E., Kinlan, B. P., & Weiss, J. M. (2007). Temperature control of larval dispersal and the implications for marine ecology, evolution, and conservation. *Proceedings of the National Academy of Sciences of the United States of America*, *104*(4), 1266–1271. https://doi.org/10.1073/pnas.0603422104

Pechenik, J. A. (1999). On the advantages and disadvantages of larval stages in benthic marine invertebrate life cycles. *Marine Ecology Progress Series*, *177*, 269–297. https://doi.org/10.3354/meps177269

Pecorino, D., Lamare, M. D., Barker, M. F., & Byrne, M. (2013). How does embryonic and larval thermal tolerance contribute to the distribution of the sea urchin *Centrostephanus rodgersii* (Diadematidae) in New Zealand? *Journal of Experimental Marine Biology and Ecology*, *445*, 120–128. https://doi.org/10.1016/j.jembe.2013.04.013

Pelletier, G., Lewis, E., & Wallace, D. (2012). *co2.sys2.1.xls, a calculator for the CO2 system in seawater for Microsoft Excel/VBA,Washington State Department of Ecology, Olympia, WA, Brookhaven National Laboratory, Upton, NY.*

Pineda, J., Hare, J. A., & Sponaugle, S. (2007). Larval transport and dispersal in the coastal ocean and consequences for population connectivity. *Oceanography*, *20*(SPL.ISS. 3), 22–39. https://doi.org/10.5670/oceanog.2007.27

Pineda, M. C., McQuaid, C. D., Turon, X., López-Legentil, S., Ordóñez, V., & Rius, M. (2012). Tough Adults, Frail Babies: An Analysis of Stress Sensitivity across Early Life-History Stages of Widely Introduced Marine Invertebrates. *PLoS ONE*, *7*(10). https://doi.org/10.1371/journal.pone.0046672

Pörtner, H. O., & Farrell, A. P. (2008). Physiology and Climate Change. *Science*, *322*, 690–692. Retrieved from http://epic.awi.de/epic/Main?puid=32305&lang=en

Powell, E. N., Klinck, J. M., Hofmann, E. E., & Ray, S. M. (1994). Modeling oyster populations. IV:Rates of mortality, population crashes, and management. *Fishery Bulletin*, *92*(2), 347–373.

Pritchard, C., Shanks, A., Rimler, R., Oates, M., & Rumrill, S. (2015). The Olympia Oyster *Ostrea lurida* : Recent Advances in Natural History, Ecology, and Restoration. *Journal of Shellfish Research*, *34*(2), 259–271. https://doi.org/10.2983/035.034.0207

Przeslawski, R., Byrne, M., & Mellin, C. (2015). A review and meta-analysis of the effects of multiple abiotic stressors on marine embryos and larvae. *Global Change Biology*, *21*(6), 2122–2140. https://doi.org/10.1111/gcb.12833

Rhein, M., Rintoul, S. R., Aoki, S., Campos, E., Chambers, D., Feely, R. A., … Wang, F. (2013). Observations: Ocean. *Climate Change 2013 the Physical Science Basis: Working Group I Contribution to the Fifth Assessment Report of the Intergovernmental Panel on Climate Change*, *9781107057*, 255–316. https://doi.org/10.1017/CBO9781107415324.010

Scheltema, R. S. (1971). Larval Dispersal as a Means of Genetic Exchange between Geographically Separated Populations of Shallow-Water Benthic Marine Gastropods. *Biological Bulletint*, *140*(2), 284–322.

Shanks, A. L. (2009). Duration and Dispersal Distance. *Biological Bulletin*, *216*(3), 373–385. https://doi.org/10.2307/25548167

Shanks, A. L., Grantham, B. A., & Carr, M. H. (2003). Propagule dispersal distance and the size and spacing of marine reserves. *Ecological Applications*, *13*(1 SUPPL.), 159–169.

Silliman, K. (2019). Population structure, genetic connectivity, and adaptation in the Olympia oyster (*Ostrea lurida*) along the west coast of North America. *Evolutionary Applications*, *12*(5), 923–939. https://doi.org/10.1111/eva.12766

Sunday, J. M., Bates, A. E., & Dulvy, N. K. (2012). Thermal tolerance and the global redistribution of animals. *Nature Climate Change*, *2*(9), 686–690. https://doi.org/10.1038/nclimate1539

Swearer, S. E., Shima, J. S., Hellberg, M. E., Thorrold, S. R., Jones, G. P., Robertson, D. R., … Warner, R. R. (2002). Evidence of self-recruitment in demersal marine populations. *Bulletin of Marine Science*, *70*(1 SUPPL.), 251–271.

Talmage, S. C., & Gobler, C. J. (2011). Effects of elevated temperature and carbon dioxide on the growth and survival of larvae and juveniles of three species of northwest Atlantic bivalves. *PLoS ONE*, *6*(10). https://doi.org/10.1371/journal.pone.0026941

Waldbusser, G. G., Gray, M. W., Hales, B., Langdon, C. J., Haley, B. A., Gimenez, I., … Hutchinson, G. (2016). Slow shell building, a possible trait for resistance to the effects of acute ocean acidification. *Limnology and Oceanography*, *61*(6), 1969–1983. https://doi.org/10.1002/lno.10348

Waldbusser, G. G., Hales, B., Langdon, C. J., Haley, B. A., Schrader, P., Brunner, E. L., … Gimenez, I. (2015). Saturation-state sensitivity of marine bivalve larvae to ocean acidification. *Nature Climate Change*, *5*(3), 273–280. https://doi.org/10.1038/nclimate2479

Wasson, K., Hughes, B. B., Berriman, J. S., Chang, A. L., Deck, A. K., Dinnel, P. A., … Zacherl, D. C.

(2016). Coast-wide recruitment dynamics of Olympia oysters reveal limited synchrony and multiple predictors of failure. *Ecology*. https://doi.org/10.1002/ecy.1602

Supplementary Materials

Supplementary Table 1: Values for 50 experimental treatments averaged over the duration of each cup's involvement in the experiment (3-17 days) with ± SD for each value.

Cup Label	Temperature (°C)	Salinity (PSU)	pH	pCO_2 (ppm)	Ω Ar	DIC (µmol / kg)
A1	14.53 ± 1.7	27.27 ± 0.7	8.06 ± 0.01	362.51 ± 11.05	1.91 ± 0.06	1881.58 ± 27.2
A2	13.67 ± 0.88	37.98 ± 0.29	7.87 ± 0.05	645.38 ± 27.9	1.87 ± 0.38	2281.12 ± 37.98
A3	13.05 ± 0.35	24.63 ± 0.26	7.81 ± 0.11	667.54 ± 192.74	1 ± 0.2	1869.27 ± 24.63
A4	13.8 ± 1.56	32.94 ± 0.33	7.71 ± 0.06	978.49 ± 153.42	1.18 ± 0.13	2273.43 ± 32.94
A5	13.4 ± 0.36	30.27 ± 0.06	8.04 ± 0.03	391.84 ± 32.87	1.98 ± 0.11	1981.31 ± 30.27
B1	14.12 ± 0.77	18.66 ± 0.1	7.66 ± 0.04	818.34 ± 64.24	0.52 ± 0.03	1550.27 ± 18.66
B2	14.22 ± 1.64	13.77 ± 2.21	7.72 ± 0.04	732.91 ± 66.45	0.5 ± 0.11	1506.84 ± 13.77
B3	14.15 ± 1.46	33.99 ± 3.41	7.87 ± 0.03	649.05 ± 29.25	1.7 ± 0.28	2213.54 ± 33.99
B4	13.35 ± 0.35	15.8 ± 0.39	7.72 ± 0.03	722.02 ± 26.1	0.53 ± 0.07	1539.42 ± 15.8
B5	13.67 ± 0.7	21.32 ± 0.03	7.98 ± 0.05	406.71 ± 55.29	1.23 ± 0.11	1676.14 ± 21.32
C1	18.58 ± 0.59	14.21 ± 2.24	7.59 ± 0.03	918.9 ± 84.17	0.4 ± 0.09	1355.29 ± 14.21
C2	18.27 ± 0.15	15.81 ± 0.08	7.9 ± 0.05	471.32 ± 68.34	0.95 ± 0.08	1484.76 ± 15.81
C3	18.6 ± 0.69	35.83 ± 0.57	8.08 ± 0.02	363.77 ± 19.37	3.07 ± 0.3	2082.06 ± 35.83
C4	17.94 ± 1.91	21.64 ± 0.17	7.64 ± 0.04	926.82 ± 88.65	0.7 ± 0.06	1683.15 ± 21.65
C5	18.38 ± 1.72	26.93 ± 0.23	8.02 ± 0.02	385.4 ± 26.09	2 ± 0.12	1805.93 ± 26.93
D1	18.98 ± 0.96	38.62 ± 0.2	7.73 ± 0.06	1038.91 ± 135.38	1.86 ± 0.25	2530.58 ± 38.62
D2	18.15 ± 0.07	34.03 ± 0.15	7.77 ± 0.02	850.67 ± 70.7	1.63 ± 0.01	2270.58 ± 34.03
D3	19 ± 0.89	18.76 ± 0.11	7.74 ± 0.03	715.11 ± 42.53	0.78 ± 0.05	1571.28 ± 18.76
D4	18.55 ± 1.55	24.12 ± 0.42	7.66 ± 0.03	964.79 ± 79.56	0.88 ± 0.08	1865.15 ± 24.12
D5	19.04 ± 0.93	29.9 ± 0.45	7.71 ± 0.02	886.53 ± 42.44	1.22 ± 0.05	2008.19 ± 29.9
E1	20.77 ± 1.15	29.83 ± 0.58	8.05 ± 0.02	370.51 ± 22.76	2.54 ± 0.1	1876.01 ± 29.93
E2	21.65 ± 0.24	33.22 ± 0.53	7.68 ± 0.03	1078.68 ± 83.8	1.49 ± 0.09	2260.58 ± 33.22
E3	21.03 ± 0.9	27.11 ± 0.45	7.63 ± 0.03	1083.7 ± 73.06	1 ± 0.09	1949.39 ± 27.2
E4	21.57 ± 0.25	24.92 ± 0.06	7.7 ± 0.01	893.76 ± 19.41	1.1 ± 0.03	1872.38 ± 24.92
E5	21.25 ± 0.79	21.72 ± 0.25	7.64 ± 0.06	1026.1 ± 134.63	0.85 ± 0.09	1806.31 ± 21.72
F1	21.63 ± 0.25	39.02 ± 0.18	7.8 ± 0.05	887.29 ± 75	2.37 ± 0.32	2516.56 ± 39.02
F2	21.6 ± NA	12.93 ± NA	7.7 ± NA	737.68 ± NA	0.56 ± NA	1349.46 ± 12.93
F3	21.09 ± 1	18.44 ± 0.3	7.98 ± 0.02	406.76 ± 25.1	1.43 ± 0.14	1553.74 ± 18.52
F4	21.62 ± 0.27	36.34 ± 0.33	7.86 ± 0.04	690.39 ± 28.77	2.32 ± 0.31	2249.3 ± 36.34
F5	21.6 ± 0.2	15.81 ± 0.34	7.68 ± 0.04	872.8 ± 86.13	0.71 ± 0.07	1601.65 ± 15.81
G1	26.23 ± 0.72	13.29 ± 0.25	7.65 ± 0.01	847.26 ± 41.14	0.63 ± 0.03	1370.82 ± 13.29
G2	26.52 ± 0.52	21.04 ± 1.42	7.74 ± 0.02	738.53 ± 38.22	1.2 ± 0.13	1629.59 ± 21.04
G3	25.7 ± 1.39	19.05 ± 0.59	7.99 ± 0.04	397.33 ± 57.34	1.82 ± 0.15	1558.96 ± 19.05
G4	26.57 ± 0.58	33.62 ± 0.33	7.75 ± 0.04	895.3 ± 79.04	2.02 ± 0.12	2159.81 ± 33.62
G5	26.6 ± 0.61	30.52 ± 0.06	7.91 ± 0.12	563.93 ± 181.29	2.48 ± 0.55	1929.4 ± 30.52
H1	26.25 ± 0.73	16.07 ± 0.13	7.64 ± 0.04	991.17 ± 75.4	0.79 ± 0.08	1600.56 ± 16.07
H2	26.48 ± 0.55	28.43 ± 0.31	7.69 ± 0.03	957.28 ± 67.96	1.49 ± 0.09	1966.96 ± 28.43
H3	26.26 ± 0.57	24.97 ± 0.23	7.78 ± 0.03	734.55 ± 55.48	1.54 ± 0.09	1808.31 ± 24.97
H4	26.25 ± 0.87	39.9 ± 0.56	7.69 ± 0.05	1140.5 ± 95.24	2.29 ± 0.42	2508.28 ± 39.9
H5	26.55 ± 0.48	36.97 ± 0.36	7.66 ± 0.03	1205.3 ± 26.04	1.93 ± 0.2	2391.48 ± 36.97
I1	28.98 ± 1.33	19.31 ± 0.51	7.72 ± 0.05	817.17 ± 116.31	1.23 ± 0.07	1654.23 ± 19.31
I2	29.45 ± 0.76	31.3 ± 0.26	7.76 ± 0.05	800.5 ± 113.17	2.07 ± 0.17	1970.09 ± 31.3
I3	29.2 ± 0.83	34.08 ± 0.78	7.71 ± 0.08	992.82 ± 210.96	2.07 ± 0.25	2145.07 ± 34.08
I4	29.65 ± 0.21	13.63 ± 0.28	7.88 ± 0.02	533.45 ± 33.63	1.28 ± 0	1433.86 ± 13.63
I5	29.38 ± 0.61	25.1 ± 0.19	7.63 ± 0.01	1123.29 ± 46	1.33 ± 0.05	1920.18 ± 25.1
J1	28.88 ± 0.9	28.62 ± 0.69	7.7 ± 0.01	927.55 ± 35.11	1.67 ± 0.05	1946.18 ± 28.62
J2	28.42 ± 1.22	22.36 ± 0.37	7.99 ± 0.05	411.59 ± 56.5	2.28 ± 0.15	1635.99 ± 22.36
J3	28.96 ± 0.79	34.98 ± 4.14	7.82 ± 0.06	730.55 ± 83.26	2.61 ± 0.6	2100.77 ± 34.98
J4	28.85 ± 0.93	39.5 ± 0.79	7.75 ± 0.03	929.75 ± 31.98	2.68 ± 0.38	2357.61 ± 39.5
J5	28.8 ± 1.24	16.41 ± 0.42	7.93 ± 0.01	460.82 ± 31.8	1.57 ± 0.06	1473.59 ± 16.41

Supplementary Table 2: Model selection process for growth model. Larval growth rate (Gr) is predicted using temperature (Temp), salinity (Sal), pH, pCO_2, and aragonite saturation (Ar). Bolded text in the model formulas represents predictors with individual p values <0.05. AIC, BIC, and R^2 were primarily used for model comparison. The last model listed is the final model chosen.

Formula	df	AIC	BIC	Adj. R^2	p
Gr ~ **Temp** + Sal + pH + Ar + pCO_2	44	271.00	284.38	0.52	<<0.001
Gr ~ **Temp** + **Sal** + Ar	46	267.06	276.62	0.57	<<0.001
Gr ~ **Temp** + **Sal** + pCO_2	46	267.00	276.56	0.57	<<0.001
Gr ~ **Temp** + **Sal** + pH	46	267.00	276.57	0.57	<<0.001
Gr ~ **Temp** + **Sal**	47	265.57	273.12	0.57	<<0.001
Gr ~ Temp + Sal + **Temp*Sal**	46	260.58	270.14	0.59	<<0.001
Gr ~ **Temp** + **Sal** + **Sal^2**	46	253.69	263.26	0.65	<<0.001
Gr ~ **Temp** + **Sal** + **Sal^2** + pH	45	253.61	265.08	0.66	<<0.001
Gr ~ Temp + $Temp^2$ + Sal + Sal^2 + Temp*Sal	41	248.02	267.15	0.71	<<0.001
Gr ~ Temp + **Sal** + **Sal^2** + **Temp*Sal** + pH	44	246.02	259.40	0.71	<<0.001
Gr ~ Temp + **Sal** + **Sal^2** + **Temp*Sal**	45	244.47	255.94	0.71	<<0.001

Supplementary Table 3: Model selection for habitat suitability. Suitability was modeled with a binomial family logistic multiple regression using temperature (Temp), salinity (Sal), pH, pCO_2, and aragonite saturation (Ar) as predictor variables. Bolded text in model formulas signifies individual predictor p values <0.05. Model comparisons used AIC, BIC, and Pseudo R^2. The last model listed is the final chosen model for habitat suitability.

Formula	AIC	BIC	Pseudo R^2	Pseudo p
Suitability ~ Temp + Sal + pH + pCO_2 + Ar	56.545	68.02	0.10	<0.01
Suitability ~ **Temp** + Sal + pCO_2	53.318	60.97	0.15	<0.001
Suitability ~ **Temp** + **Sal** + pH	53.293	60.94	0.15	<0.001
Suitability ~ **Temp** + **Sal** + Ar	52.959	60.61	0.16	<0.001
Suitability ~ Temp + Sal + Temp * Sal	52.944	60.59	0.16	<0.001
Suitability ~ **Temp** + **Sal**	51.849	57.59	0.17	<0.001
Suitability ~ **Sal** + **Sal^2**	44.477	50.21	0.29	<<0.001
Suitability ~ Temp + **Sal** + $Temp^2$ + **Sal^2**	22.551	32.11	0.64	<<0.001
Suitability ~ Temp + **Sal** + **Sal^2** + Temp * Sal	21.825	31.38	0.65	<<0.001
Suitability ~ **Temp** + **Sal** + **Sal^2**	20.553	28.20	0.67	<<0.001

Supplementary Table 4: Case study field data from two restoration sites in Washington State between the years 2014 and 2019. Field data are listed on the left, and modeled response variables on the right of the vertical line. "SEA" label denotes data sourced from the WWU SEA Discovery Center in Poulsbo, WA. "McIntyre" signifies from McIntyre et al (in revision), and "Cordoba" from Cordoba and Arellano, unpublished data.

Site	Year	°C	PSU	Dates	Source	Growth Rate (µm/day)	PLD (days)	Habitat Suitability Likelihood %
Liberty Bay	2017	16.44 ± 0.59	29.09 ± 0.58	Jul. 7 – Aug 23	SEA	5.61	18.53	31.12
Liberty Bay	2018	17.36 ± 1.15	29.58 ± 2.43	Jul. 7 – Aug 23	SEA	6.15	16.90	49.9
Liberty Bay	2019	16.71 ± 1.07	27.7 ± 0.81	Jul. 7 – Aug 23	SEA	5.78	17.98	26.65
Fidalgo Bay	2017	16.6 ± 1.3	29 ± NA	Jul. 11-14	McIntyre	5.71	18.20	33.66
Fidalgo Bay	2014	16.5 ± 0.5	28.4 ± 0.25	Jul. 2, 14	Cordoba	5.67	18.35	28.8

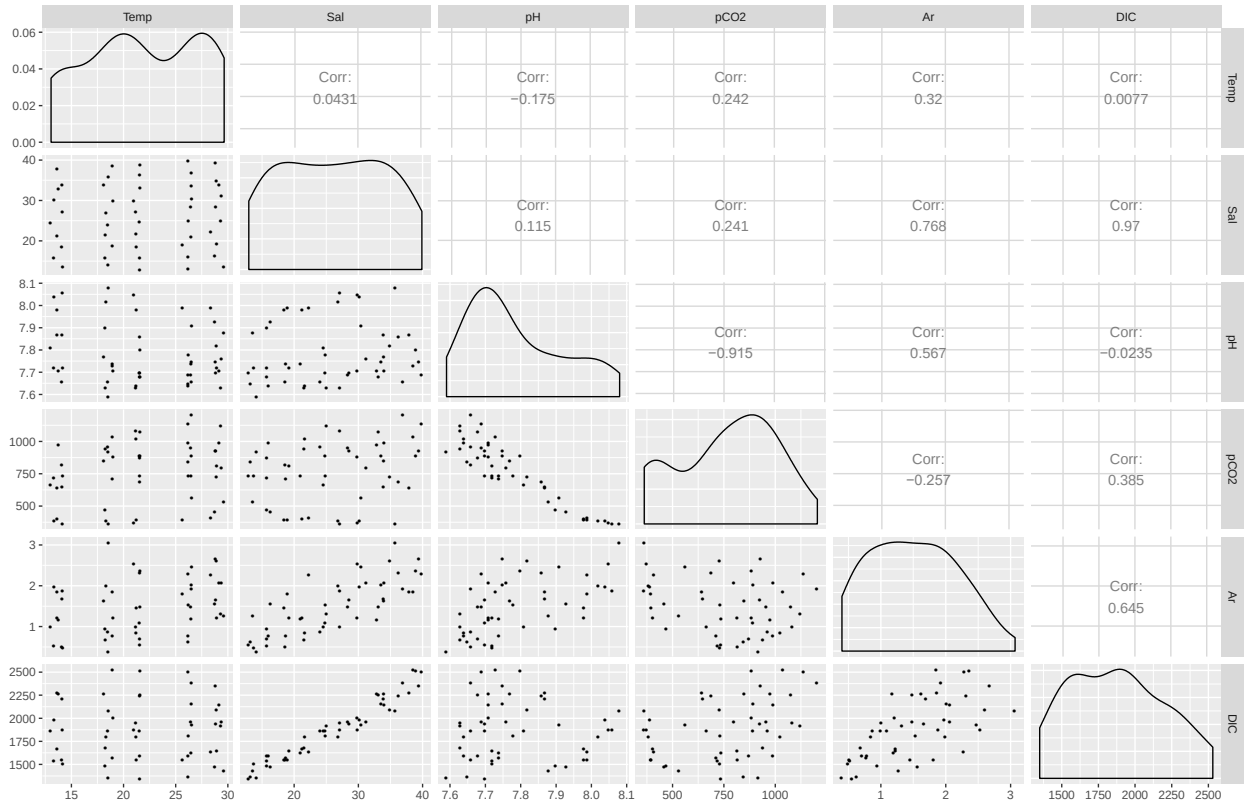

Supplementary Figure 1: Correlation matrix of predictor variables in larval growth and habitat suitability models.

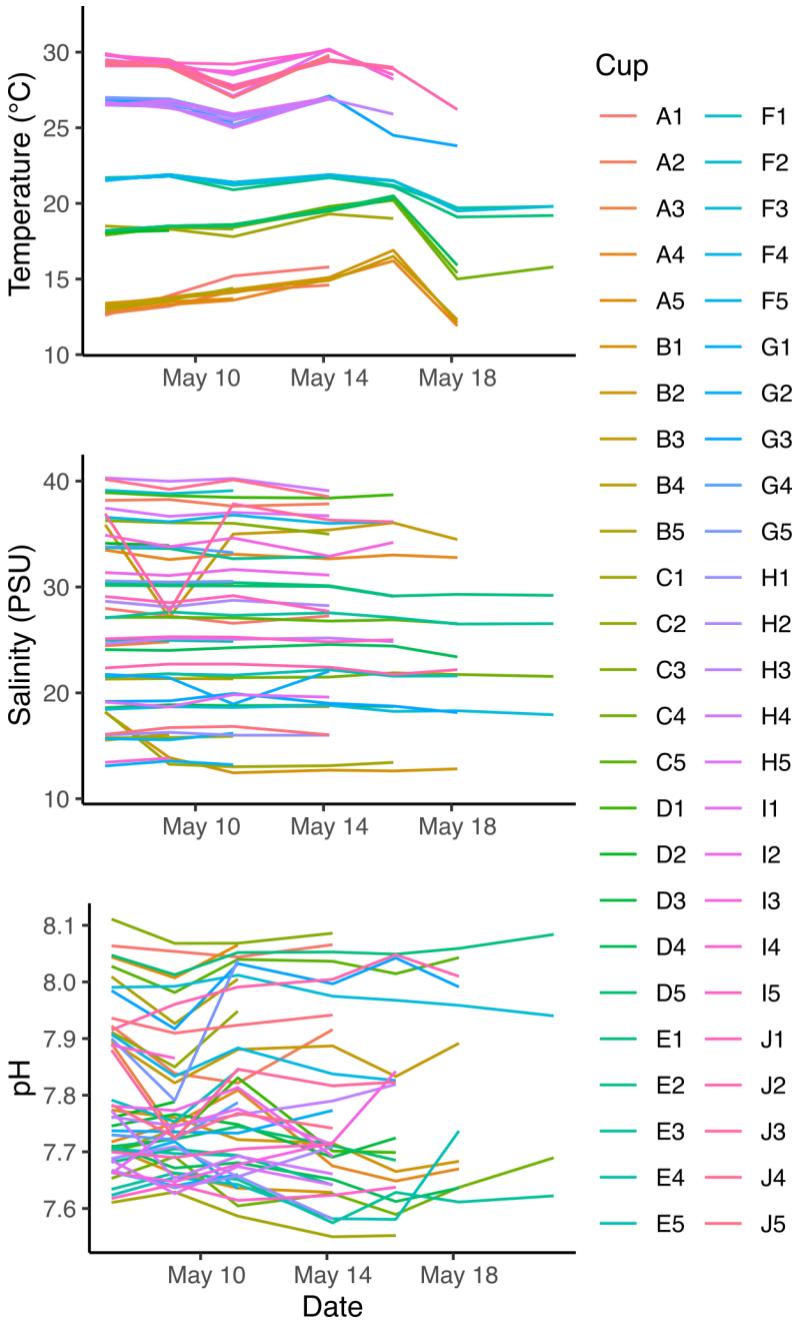

Supplementary Figure 2: Treatment cup variable stability over time from May 7 to May 21, 2018.

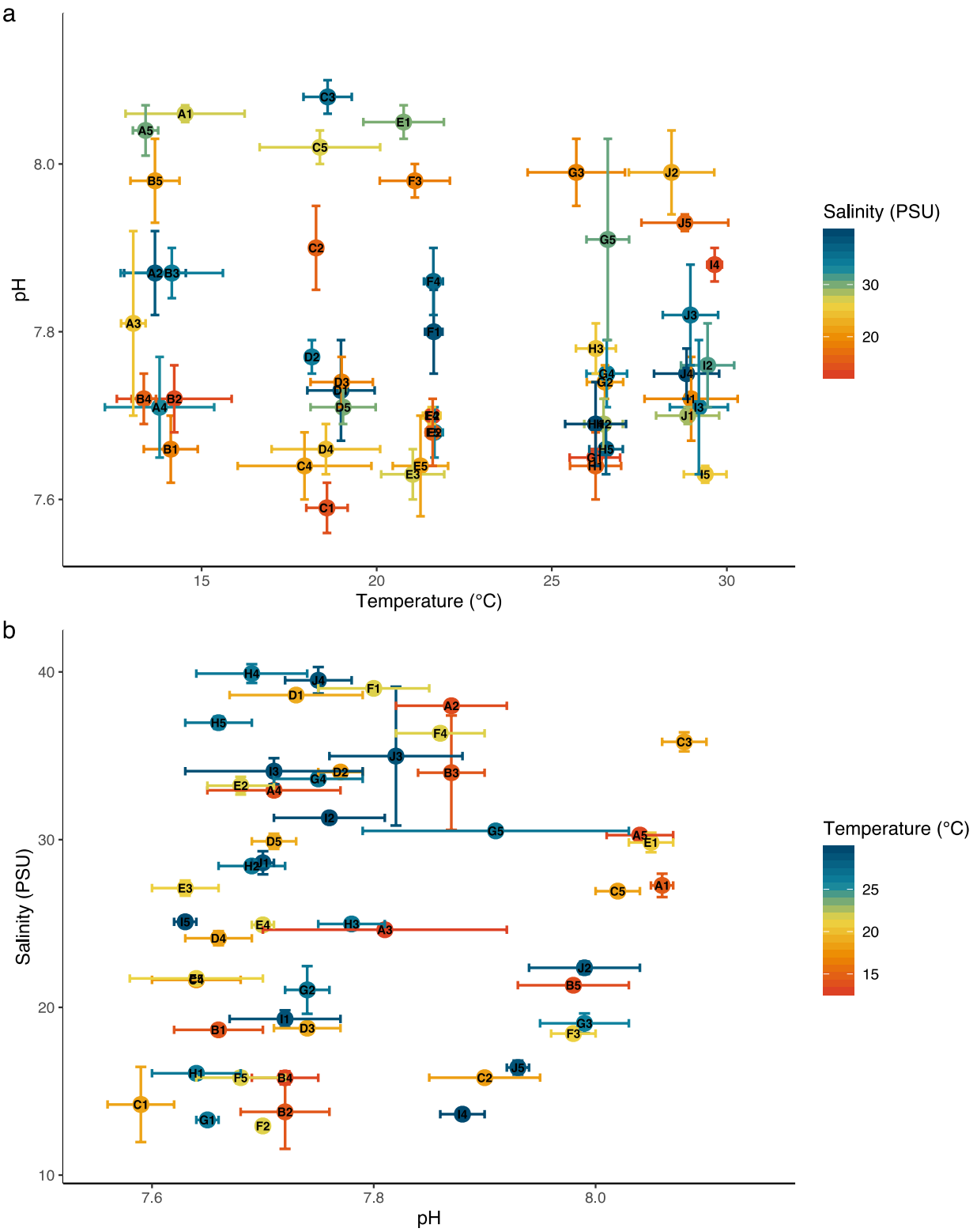

Supplementary Figure 3: average treatment values of culture cups in the experiment organized by temperature and pH (a), and pH and salinity (b) as addendum to Fig 2, arranged by salinity and temperature. Error bars represent the standard deviation of axis variables for the duration of the cup's inclusion in the experiment (3-17 days).

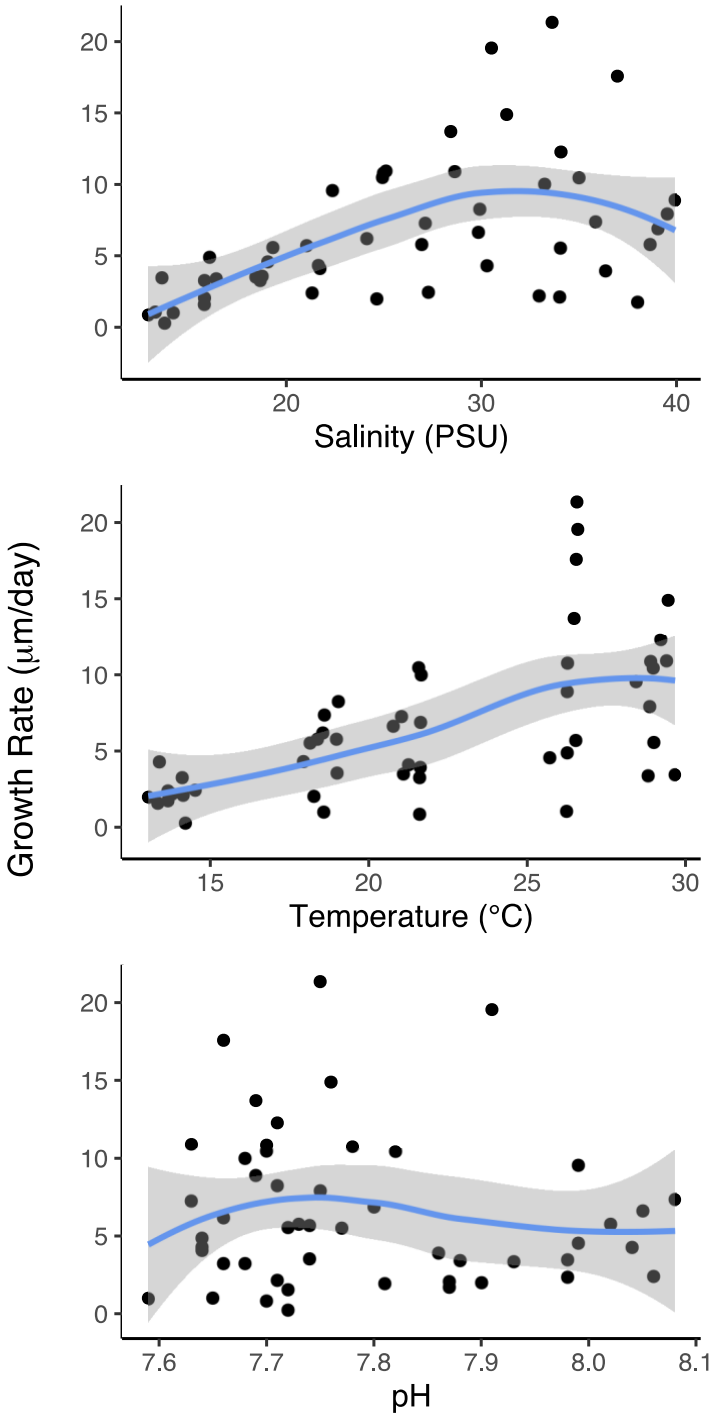

Supplementary Figure 4: Experimental growth rate distribution by variable with loess curve fits.

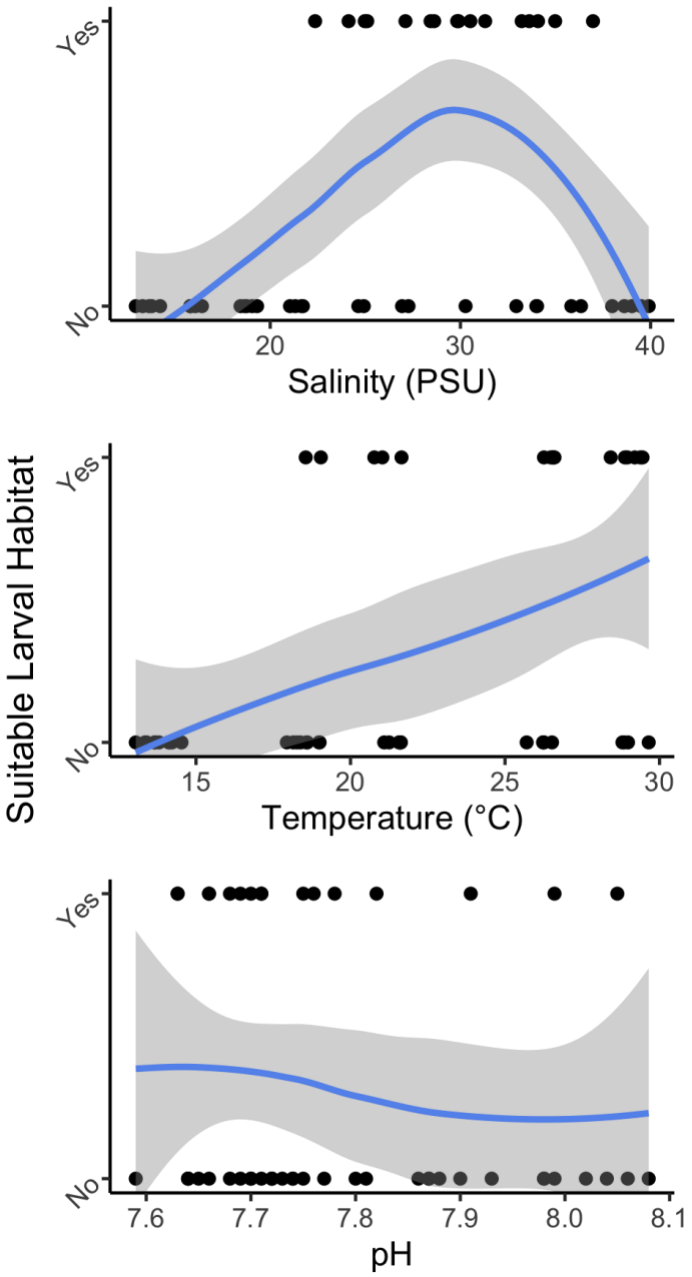

Supplementary Figure 5: Experimental habitat suitability by variable with loess curve fits.